NORWEGIAN JOURNAL OF GEOLOGY
https://dx.doi.org/10.1785/njg100-1-6

GEOLOGICAL SOCIETY OF NORWAY

Late Neoproterozoic basin evolution of the magma-rich Iapetus margin of Baltica

Hans Jørgen Kjøll[1]

[1]Centre for Earth Evolution and Dynamics (CEED), Department of Geosciences, University of Oslo, Norway.

E-mail corresponding author (Hans Jørgen Kjøll): h.j.kjoll@geo.uio.no

Keywords:
- Stromatolites
- Glaciogenic diamictite
- Seve Nappe Complex
- Rifting
- Continental breakup
- Caledonides

Received:
31. March 2020

Accepted:
5. April 2020

Published online:
9. June 2020

Electronic Supplement 1:
Clast distribution

Electronic Supplement 2:
Analytical data detrital zircon

Electronic Supplement 3:
Analytical data HJK_2026

Electronic Supplement 4:
Methods

The Särv and Seve nappe complexes (NC) in the central and northern Scandinavian Caledonides locally display well-preserved, mafic dyke-intruded sedimentary successions commonly interpreted to have been deposited in sag- to rift basins along the margin of the Iapetus Ocean. The sedimentary successions are generally interpreted to have been deposited prior to or during the Late Neoproterozoic opening of the Iapetus Ocean. They were later incorporated into the Scandinavian Caledonides during the Silurian-aged Scandian orogeny. Whereas the minimum depositional age is constrained by the dated mafic dyke swarm at c. 596–608 Ma, a maximum depositional age for the sedimentary successions is poorly constrained. No fossils or diamictite units have hitherto been reported from the sedimentary successions found in the Seve NC. This contribution presents new geological observations and geochronological data from allochthonous, dyke-intruded, rift-related basins. Key elements in the sedimentary succession, such as carbonates with meta-evaporitic domains, diamictite and stromatolites are described from the Särv and Seve NC. Evidence presented here suggests that the diamictite is of glaciogenic origin. It is cut by the dykes and is therefore older than 608 Ma and could be related to the Marinoan or Sturtian glaciations. The stromatolite resembles *Eleonora laponica* and is found below the diamictite. Two field areas have young detrital zircons of c. 700–750 Ma providing possible upper maximum depositional ages and thus bracket the deposition within a c. 100 M.yr. time interval between 700 and 608. This is corroborated by a Palaeoproterozoic orthogneiss with a 631 Ma Pb-loss event, possibly reflecting the development of a top-west, ductile extensional shear fabric and frictional co-seismic deformation. This extensional event generated accommodation space at the surface and thus basin formation. Similarities between the separate basins, like the highly dyke-intruded nature, the similarities in contact and regional metamorphism as well as the detrital zircon age distributions, suggest that the basins are related.

Introduction

The geological record preserved on Baltica and Laurentia from the end of Sveconorwegian/Grenvillian time to the Caledonian continent-continent collision has many unresolved questions (e.g., Jakob et al., 2019; Slagstad et al., 2019). One pertinent question, which has the potential to influence the architecture of the Scandinavian Caledonides, deals with the rifted margin framework of the Baltican and Laurentian Iapetus margins (e.g., Jakob et al., 2019). Factors such as when the rifting initiated are difficult to constrain because of metamorphic overprint and by the scarcity of Neoproterozoic tectonomagmatic zircon-

Kjøll, H.J. 2020: Late Neoproterozoic basin evolution of the magma-rich Iapetus margin of Baltica. *Norwegian Journal of Geology 100*, 202005, https://dx.doi.org/10.17850/njg100-1-6.

producing events. Several Cryogenian and Ediacaran ages have been reported for single detrital zircon analyses from metasedimentary rocks of the Särv and deformed parts of the Seve NC (e.g., Be'eri-Shlevin et al. 2011; Kirkland et al., 2011; Gee et al., 2014), but no detrital ages have been presented from the well-preserved, heavily dyke-intruded sedimentary successions of the Seve NC (e.g., Svenningsen, 1994a; Stølen, 1994).

A number of studies have been conducted both in the Särv and Seve NC focusing on the rift-related sedimentary successions, representing the ocean-continent transition (e.g., Kumpulainen, 1980; Kathol, 1989; Svenningsen 1994a; Stølen, 1994) and on the lower non-dyked allochthons, representing the more proximal part of the margin (e.g., Nystuen, 1987; Plink-Björklund et al., 2005; Nystuen et al., 2008). Based on similarities between the sedimentary successions and the amount of dyking, most of these studies suggest a lateral correlation between the dyke-intruded (here termed dyked) and dyke-lacking (here termed non-dyked) basins, along strike of the orogen (e.g., Stølen 1994; Andréasson et al., 1998; Plink-Björklund et al., 2005).

Diamictites in Neoproterozoic sedimentary strata may be linked to global glaciations and can thus serve as key time markers and stratigraphic units for correlations (e.g., Kirschvink, 1992; Hoffman et al., 1998; Hyde et al., 2000; Hoffman & Schrag, 2002; Halverson et al., 2005). Commonly, three major glaciation events are recognised, the Sturtian (c. 712 Ma, Allen et al., 2002), Marinoan (c. 635 Ma, Hoffmann et al., 2004) and the Gaskiers (c. 580 Ma, Bowring et al., 2003; Pu et al., 2016). There is, however, still some controversy regarding the actual extent and duration of these major events and whether there were several smaller events as well (e.g., Eyles & Januszczak, 2004; Kendall et al., 2006; Allen & Etienne, 2008; Le Heron et al., 2019). On Baltica, several diamictite units have been described, e.g., from the Gaissa basin in the Tana–Varangerfjorden area, Finnmark (Reusch, 1891; Edwards, 1984; Zhang et al., 2016), Risbäck (Plink-Björklund et al., 2005; Kumpulainen & Greiling, 2011) and the Hedmark basin (Holtedahl, 1922; Nystuen, 1976; Bingen et al., 2005; Nystuen & Lamminen, 2011), where they are non-dyked, and from the Tossåsfjället basin (Kumpulainen, 1980; Kumpulainen et al., 2016; Nystuen et al., 2016), where they are dyked. No such observations have hitherto been described in the literature from the heavily dyke-intruded Seve NC making a correlation more challenging.

Because of the locally pervasive Caledonian metamorphic and structural overprint, few studies have dealt with the extensional processes that led to the opening of the Iapetus Ocean (e.g., Svenningsen, 1994a; Andréasson et al., 1998; Andersen et al., 2012; Jakob et al., 2019; Kjøll et al., 2019a, b). Thorough knowledge of the rift processes has been shown to be important for the understanding of the subsequent orogenic events, as rift structures may be reactivated and therefore partly control the final geometry of the mountain belt (e.g., Mohn et al., 2011; Beltrando et al., 2014; Epin et al., 2017; Jakob et al., 2019). Having an understanding of the tectonostratigraphy may therefore aid in getting a better understanding of the architectural elements of the pre-orogenic rifted margin.

This contribution aims to better constrain the temporal evolution of the pre-Caledonian margin of Baltica, using the youngest detrital zircon grains from the sedimentary succession to assess the timing of sedimentation of the heavily dyked sedimentary successions in the Seve NC. Furthermore, new, and possibly the first, observations of columnar stromatolites and a possibly glaciogenic or glacially influenced diamictite unit from the Seve NC are presented. Lastly, this paper presents geochronological data from a basement orthogneiss with a top-W extensional fabric that shows that the zircons underwent Pb loss at 631 Ma, which is interpreted to show that the Baltican crust underwent stretching at that time. Together, these new observations and analytical data help to constrain the timing of stretching deposition of the heavily dyked sedimentary succession preserved in the Seve NC.

Geological setting

This section introduces the geological setting starting with the Neoproterozoic rifting of Baltica and Laurentia and subsequent basin formation, before describing the inversion of the margin during the Caledonian continent-continent collision.

Neoproterozoic rifting and break-up

Most paleogeographic models place Baltica and Laurentia in close proximity to each other in the postulated supercontinent Rodinia in the Early Neoproterozoic (e.g., Li et al., 2008; Pease et al., 2008; Merdith et al., 2017; Tegner et al., 2019). There are, however, some uncertainties in the configuration of the continents and new continental arrangements have recently been proposed, challenging the commonly accepted plate configurations for the Neoproterozoic (Slagstad et al., 2019).

Thick, primarily clastic, sedimentary successions are preserved in the Scandinavian Caledonides. These were deposited in the Late Tonian or Early Cryogenian in wide and extensive sag-basins that developed into narrow rift basins during the progressive opening of the Iapetus Ocean (Nystuen et al., 2008). It has been proposed that the margin of Baltica developed into a wide and segmented margin with a southern (present-day coordinates) magma-poor segment and a northern magma-rich segment (e.g., Kumpulainen & Nystuen 1985; Andersen et al., 2012; Abdelmalak et al., 2015; Jakob et al., 2017, 2019; Kjøll et al., 2019a). The northern segment became magma-rich during the final break-up of Baltica and Laurentia, which was marked by voluminous magmatism, related to elevated mantle potential temperatures, i.e., a mantle plume. Evidence for this major tectonomagmatic event is found as a c. 1000 km-long dyke complex (Kjøll et al., 2019a; Tegner et al., 2019). This dyke complex was emplaced over a large area during a geologically short time period from 608–596 Ma (Bingen et al., 1998; Svenningsen, 2001; Baird et al., 2014; Kumpulainen et al., 2016; Kjøll et al., 2019a; Tegner et al., 2019) and caused significant heating and local migmatisation of the crust, which may have caused thermal weakening, leading to the final break-up (Kjøll et al., 2019a, b). This magmatism primarily affected the distal basins, where the dykes are cutting the entire preserved sedimentary sequence. Their crystallisation depth has been constrained to range from 8 to12 kilometres, suggesting deposition of a thick sedimentary package and/or extrusion of significant volumes of lava, consistent with observations from modern magma-rich rifted margins (Abdelmalak et al., 2015; Kjøll et al., 2019a).

Neoproterozoic basins

The Neoproterozoic sedimentary successions that were deposited on the Baltican margin and now are partially preserved in the southern and central Scandinavian Caledonides can be subdivided into two groups; 1) non-dyked Proterozoic sedimentary rocks and 2) dyked Proterozoic sedimentary rocks. The non-dyked sedimentary rocks are generally interpreted to have formed along the proximal margin of Baltica, away from the magmatic centres and are thus less affected by the volcanic activity than their dyked counterparts, which were closer to the magmatic centres (e.g., Nystuen, 1983; Jakob et al., 2019). Examples of the proximal basins are the Hedmark, Engerdalen, Risbäck, and Gaissa basins (Fig. 1). The dyked basins, on the other hand, are interpreted to have formed on the more distal margin, where the break-up-related magmatism was more intense, and where the volume of mafic magmatic rocks can vary from 50 to 100% (Kjøll et al., 2019a). Examples of heavily dyked areas are Särv (Tossås-fjället basin; Kumpulainen, 1980), Sarek (Svenningsen, 1994a), Váivvancohkka (Kathol, 1989), Indre Troms (Stølen, 1994) and Corrovarre (Zwaan & van Roermound, 1990; Fig. 1).

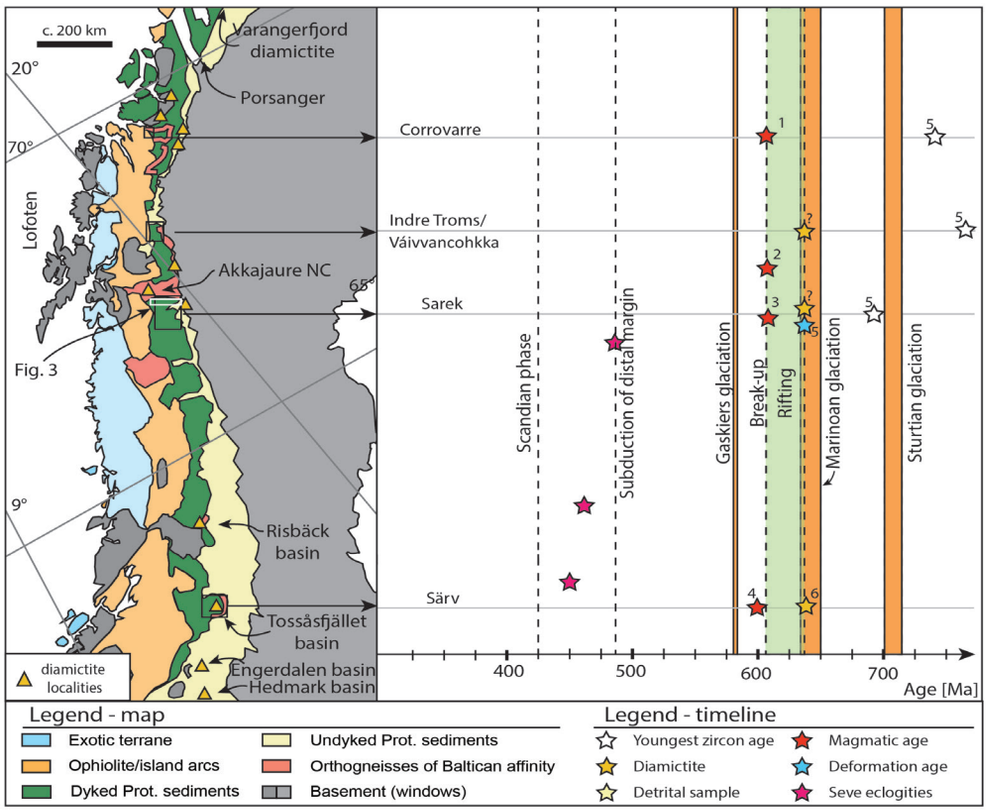

Figure 1. Simplified tectonostratigraphic map of the central Scandinavain Caledonides and schematic time-line of the rifting event recorded on Baltica. Black rectangles indicate study areas. White rectangle indicates location of map in Fig. 3A. Timeline vs. latitude diagram indicating major rifting events. 1: Kjøll et al., 2019, 2: Baird et al., 2014, 3: Svenningsen, 2001, 4: Bingen et al., 1998, 5: this study, 6: Kumpulainen, 1980.

The non-dyked, proximal basins are primarily filled with shallow-marine siliciclastic sediments that are locally succeeded by a carbonate shelf succession and diamictites. This sedimentary succession has been well documented in a number of theses and publications and the reader is therefore referred to these works for detailed descriptions of the sedimentary rocks (e.g., Kumpulainen, 1980; Kumpulainen & Nystuen, 1985; Kathol, 1989; Zwaan & von Roermound, 1990; Stølen, 1994; Svenningsen, 1994a; Lindahl et al., 2005; Plink-Björklund, 2005). A short summary of the key elements based on the published literature is provided in section 3 below.

The distal, dyked basins were filled, similarly to the non-dyked basins, with primarily, shallow-marine siliciclastic sediments overlain by a carbonate shelf succession followed by more siliciclastic sediments (e.g., Kumpulainen, 1980, Nystuen et al., 2008; Pease et al., 2008). In addition, glaciogenic diamictites are described from the Tossåsfjället basin in Särv, where they rest directly on top of the carbonate shelf succession (Kumpulainen 1980; Kumpulainen & Nystuen 1985; Fig. 2).

Main Caledonian events

During initial stages of the Caledonian orogeny, in the Early to Middle Ordovician, the Seve NC underwent amphibolite to eclogite-facies metamorphism (Fig. 1, Roberts and Gee, 1985; Root & Corfu, 2012; Corfu et al., 2014; Majka et al., 2014; Klonowska et al., 2017). During this event, kilometre-scale mega-boudins formed within the Seve NC (Albrecht, 2000). The interior of these boudins escaped most of the penetrative Caledonian deformation and metamorphism and, therefore, locally preserve

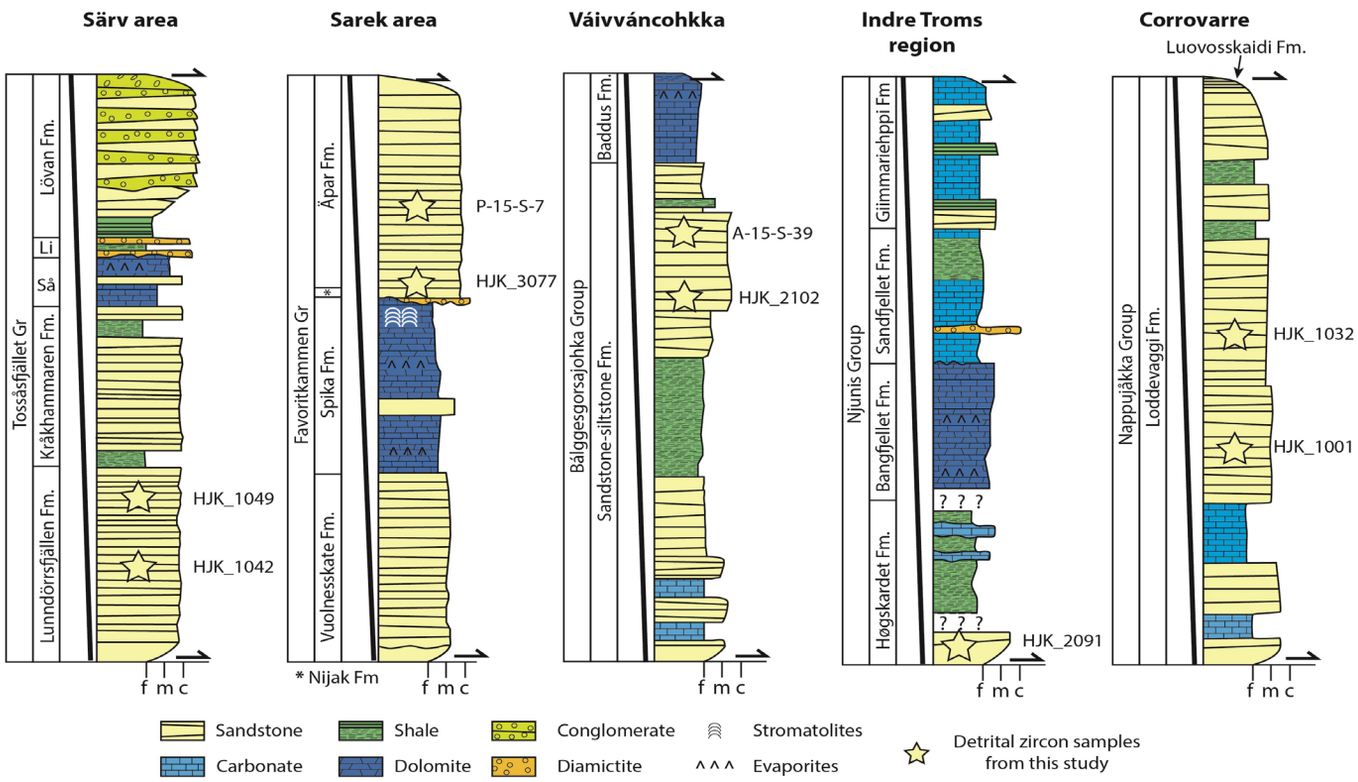

Figure 2. Schematic stratigraphy of dyke-intruded Neoproterozoic sediments of the Seve NC from all the field areas based on previously published sections. Yellow stars indicate approximate locations in the stratigraphy of the detrital zircon samples. Särv: Kumpulainen, 1980 and Kumpulainen & Nystuen, 1985, Sarek: Svenningsen, 1994, Váivvancohkka: Kathol, 1989, Indre Troms: Stølen, 1994, Corrovarre: Lindahl et al., 2005 and Zwaan & Van Roermound, 1990. Li – Lifjället Fm., Så – Storån Fm

primary sedimentary features as well as contact-metamorphic mineral assemblages formed during the emplacement of the Neoproterozoic dyke swarm (Svenningsen, 1994a; Kjøll et al., 2019a). The units were partly exhumed, imbricated and thrust onto the more proximal domain of the rift zone and the Baltican basement itself, during the Scandian phase of the collision (e.g., Andréasson et al., 2018). In Sarek (Fig. 1), these deformed units have $^{40}Ar/^{39}Ar$ plateau ages of 469 to 428 Ma, interpreted to date the imbrication and nappe emplacement (Dallmeyer et al., 1991; Svenningsen, 2000). In the Särv area (Fig. 1), the dyked basin sedimentary rocks escaped the early Caledonian subduction and were only affected by greenschist-facies metamorphism during imbrication and nappe emplacement (Gilotti & Kumpulainen, 1986). The entire tectonostratigraphy is exceptionally well preserved in the Sarek area in northern Sweden, where recent glacial erosion has exposed the tectonostratigraphy from the transition from the well-preserved mega-boudins, revealing the Neoproterozoic primary relationship between the sediments and the dykes, to the strongly deformed parts of the Seve NC and the underlying units. This tectonostratigraphy is presented in more detail in the sub-chapter below.

Tectonostratigraphy in the Sarek area

The tectonostratigraphy in Sarek shows that directly below the well-preserved mega-boudin rests a unit consisting of metasandstone and carbonate with abundant mafic boudins. This strained unit is referred to as the Mihká unit (also spelled “Mikka”, e.g. Andréasson, 1986; Rehnström et al., 2002). Below the Mihká unit rests the Akkajaure NC, which is an imbricated thrust sheet with basement-cover contacts intruded by mafic sheet intrusions that are locally boudinaged (e.g., Björklund, 1985, 1989; Rehnström et al., 2002; Kirkland et al., 2011). The cover sequence is referred to as the Skárjá unit and consists

primarily of clastic and semipelitic metasedimentary rocks (Björklund, 1989). A granitic sheet intruding the cover sequence has been dated to 1797 ± 4 Ma (Kirkland et al., 2011) and 1776 ± 4 Ma (Rehnström et al., 2002). Rehnström et al. (2002) also reported metamorphic titanites in these granitic sheets that (re)crystallised at 637 ± 3 Ma. The underlying Akkajaure NC basement rocks consist primarily of granite, syenite, anorthosite and minor gabbroic rocks with protolith ages of 1788 ± 6, 1795 ± 2, 1800 ± 2, 1806 ± 15 and 1876 ± 10 Ma (Rehnström & Corfu, 2004; Kirkland et al., 2011).

Detailed description of dyke-intruded, allochthonous rift-related sedimentary successions

In the following, the lithostratigraphies of the dyke-intruded basins in the Seve NC of the Scandinavian Caledonides are reviewed. These areas have been suggested to constitute the transitional crust of Baltica (e.g., Andréasson, 1994; Svenningsen, 2001; Kjøll et al., 2019a, b) and comprise between 50 and 90% mafic dykes (Kjøll et al., 2019a). Bases and tops of the sedimentary successions were tectonically deformed during Caledonian nappe emplacement; therefore, only a minimum estimate of the total sedimentary thickness can be reported. The areas are presented from the south to the north (Fig. 1).

Särv

The Särv area (Fig. 1) comprises the Tossåsfjället Group (Kumpulainen, 1980, 2011, Fig. 2), which has a preserved thickness of >4 km and consists of five formations. The Lunndörsfjällen Formation (Fm) is the lowest one and consists primarily of arkosic metasandstones with some thin intercalations of siltstones. The overlying Kråkhammaren Fm records a change to quartzites, siltstones and shales. The Kråkehammaren Fm is overlain by the Storån Fm, which is a c. 100 metre-thick unit dominated by dolostone locally interbedded with a quartzite unit several metres thick. The dolostone bands are thinly bedded and in places interbedded with fine-grained quartz-sandstone and mudstones (Kumpulainen, 1980, 2011). Chert nodules are locally present and are associated with meta-evaporitic magnesite deposits (Kumpulainen, 1980). This suggests that parts of the Storån Fm were formed as sabkha-type evaporitic deposits in intratidal or supratidal flats (Kumpulainen, 1980, 2011). Similar observations are also made for Särv correlatives to the west in the Engerdalen Basin in the Kvitvola Nappe (Fig. 1, Nystuen, 1969, 1980). The contact to the overlying Lillfjället Fm is described by Kumpulainen (1980) to be unconformable. The Lillfjället Fm comprises two distinct glaciogenic diamictite units separated by a more than 500 m-thick sandstone-siltstone unit; the lowermost diamictite contains dolostone clasts (Kumpulainen, 1980, 2011). The uppermost, preserved formation is the Lövan Fm, which displays alluvial feldspathic sandstones, conglomerates and sporadic siltstones (Op. cit).

Sarek

In the Sarek area of northern Sweden (Fig. 1), Svenningsen (1994b) has described the Favoritkammen Group with a preserved stratigraphic thickness of >3.6 km (Fig. 2). The group consists of three formations where the lowermost Vuolnesskalte Fm comprises a calc-silicate-rich meta-psammite. There is a transitional boundary to the overlying Spika Fm which primarily consists of dolostone with local layers of calc-arenites and metapsammite. The dolostones are intercalated with 1–5 cm-thick calc-silicate horizons. Magnesite and scapolite are disseminated within the formation. Locally, pure magnesite lenses can be found. These are interpreted to represent meta-evaporitic deposits that were mobilised during the dyke emplacement event (Svenningsen, 1994b; Kjøll et al., 2019a). Directly abo-

ve the Spika Fm, Svenningsen (1994b, 1995) described a thin conglomerate horizon with abundant granitic clasts and called it the Niak Formation. The spelling on Swedish maps has changed since then and throughout the remainder of the text the unit will be referred to as the "diamictite unit" or "Nijak Formation", consistent with the updated Swedish maps. Svenningsen (1995) further noted that the Nijak Fm is tectonically reworked and that its relationship to the under- and overlying units is uncertain. Above the Nijak Fm rests the Äpar Fm – a thick (>2.5 km) succession of shallow-marine sandstones intercalated with fine-grained argillaceous beds (Kjøll et al., 2019a). The entire 'Favoritkammen outcrop' in the type locality at Sarek is strongly affected by contact metamorphism due to the intense dyke-swarm network (Kjøll et al., 2019a, b).

Váivvancohkka

In the Váivvancohkka area (Fig. 1), Kathol (1989) described the Bálggesgorsajohka Group (Fig. 2), which contains two units, the informally named 'Sandstone-siltstone' unit and the Baddus Fm. The sandstone-siltstone unit contains primarily thickly bedded quartzites and arkoses, and laminated siltstones. The Baddus Fm is described as a carbonate unit with distinct contact-metamorphic scapolite, diopside and garnet-bearing bands. Conglomerates have not been described. The stratigraphic top of the Baddus Fm is not exposed or preserved in the Váivvancohkka area.

Indre Troms

In Indre Troms (Fig. 1), Stølen (1994) described the Njunis Group (Fig. 2), consisting of four formations. The lowermost one, the Høgskardet Fm, consists of graphitic schists and fine-grained arkoses. This formation is overlain by the Bangfjellet Fm which comprises a several hundred metre-thick dolostone unit which is intercalated with 2–8 cm-thick calc-silicate layers. Directly above the Bangfjellet Fm, separated by a local angular unconformity, rests the Sandfjellet Fm. This formation consists of calcareous schist and impure marbles with calc-silicate bands and Cl-rich scapolite (Kjøll et al., 2019a). Within the Sandfjellet Fm., Stølen (1994) described a conglomeratic unit consisting of granitoid pebbles in a mudstone matrix. The uppermost formation is the Giimmariehppi Fm., which comprises a marble with calc-silicate and scapolite bands.

Corrovarre

Farther north, in the Corrovarre area (Fig. 1), the pre-Caledonian metamorphism as well as Caledonian reworking is more extensive, and the area with well-preserved rocks is smaller making a clear stratigraphic subdivision difficult. Nevertheless, the Nappujåkka Group (Fig. 2) has been described and sub-divided into two formations (Zwaan & Van Roermund, 1990; Lindahl et al., 2005). The main lithology of the lowermost Loddevággi Fm is meta-arkose, which reveals transitions into more mica-rich sandstones towards the top (Zwaan et al., 1975). Thick units of calcitic marble are also present. The uppermost unit, the Luovosskaidi Fm was interpreted by Lindahl et al., (2005) to represent a more intensely deformed upper domain of the Loddevággi Formation.

New field observations from the Sarek area

Stromatolites in the Spika Fm

During fieldwork in Sarek (Fig. 1), in a glacial cirque with difficult access, a locality with columnar stromatolites was discovered towards the top of the Spika Fm (Äpar in Fig. 3). The locality is little affected by the regional metamorphism and deformation, and has abundant primary sedimentary structures, such as cross-bedding and water-escape structures indicating right way up towards the south. The host carbonate rock is a grey marble with 5–25 cm-thick beds separated by more clastic horizons (Fig. 3B). Locally, features resembling algae growth structures can be observed (Fig. 3B, C). The stromatolites are c. 30 cm tall and display branching within their dome structure, indicating that the growth rate was faster than the sediment accumulation rate (Riding, 2011). The ramification is verticillate with several branches from a central column (white dashed lines in Fig. 3C). The diameter of the individual branches varies from c. 2 to 15 cm. The growth of the branches was slightly oblique with respect to the palaeo-vertical direction (Fig. 3B, C). The curviplanar laminae of the stromatolites are convex and display several dome/basin-like features (Fig. 3C). The geometry of the stromatolite suggests that it formed through microbial precipitation in a shallow-marine setting (Riding, 2011). Where the columnar stromatolites occur, the carbonate is more light brown, in contrast to the light grey colour elsewhere (Fig. 3B). The sedimentary bedding is draping the top of the stromatolite and on-lapping to its sides. To the present author's knowledge, columnar stromatolites have not been described before in the Spika Fm, nor from elsewhere in the Seve NC.

The diamictite deposit in the Nijak Fm

In Sarek, south of peak Nijak, (Fig. 3A), between the Spika and Äpar formations, rests a thin (5–10 m) matrix-supported, polymict diamictite, first described by Svenningsen (1994b) as the Nijak Fm (Fig. 3D). The matrix consisted originally of silt and clay, now metamorphosed into a calcareous garnet-bearing mica-rich lithology with local layers of silt and fine-grained sand. Traces of a sedimentary lamination occur locally (Fig. 3D). Where the matrix presumably was particularly rich in clay it has been replaced by coarse-grained (mm-scale) muscovite, minor biotite and large (c. 1 cm in diameter) red garnets. Minor small (<1 cm long) amphibole or tourmaline needles also occur in the matrix. There are four main types of clasts ranging from 0.5 to 25 cm in diameter, where quartz-vein and amphibolite clasts are the most common (Fig. 3D and Electronic Supplement 1). Other types of clasts are dolostone, granite and gneiss as well as some that could not be determined (Fig. 3D–G and Electronic Supplement 1). Some of the clasts are foliated and some display folded foliations, testifying to metamorphism and deformation prior to transport and deposition (Fig. 3D, E). There is a clast-type distribution within the unit, where the lower part contains all clast types, whereas the top of the unit is dominated by carbonate clasts, resembling dolostone with the characteristic criss-cross weathering pattern (white lines in Fig. 3F). Along the periphery of the clasts, there are several grooves or embayments in the surface towards the fine-grained matrix (white arrows in Fig. 3F). Clast counting on field photographs indicates that c. 55% of the clasts are composed of vein quartz, 19% carbonate, 16% amphibolite, 5% granite, 1% gneiss and c. 5% with an unknown composition (Fig. 3G, Electronic Supplement 1). Thus, basement-derived clasts constitute c. 76% of the clast population. Some of the clasts are sub-rounded (Fig. 3D, G) whereas others, such as the carbonate clasts, are sub-angular (Fig. 3F). A reaction rim separating some of the clasts from the matrix obliterates the original morphology of the affected clast (Fig. 3E).

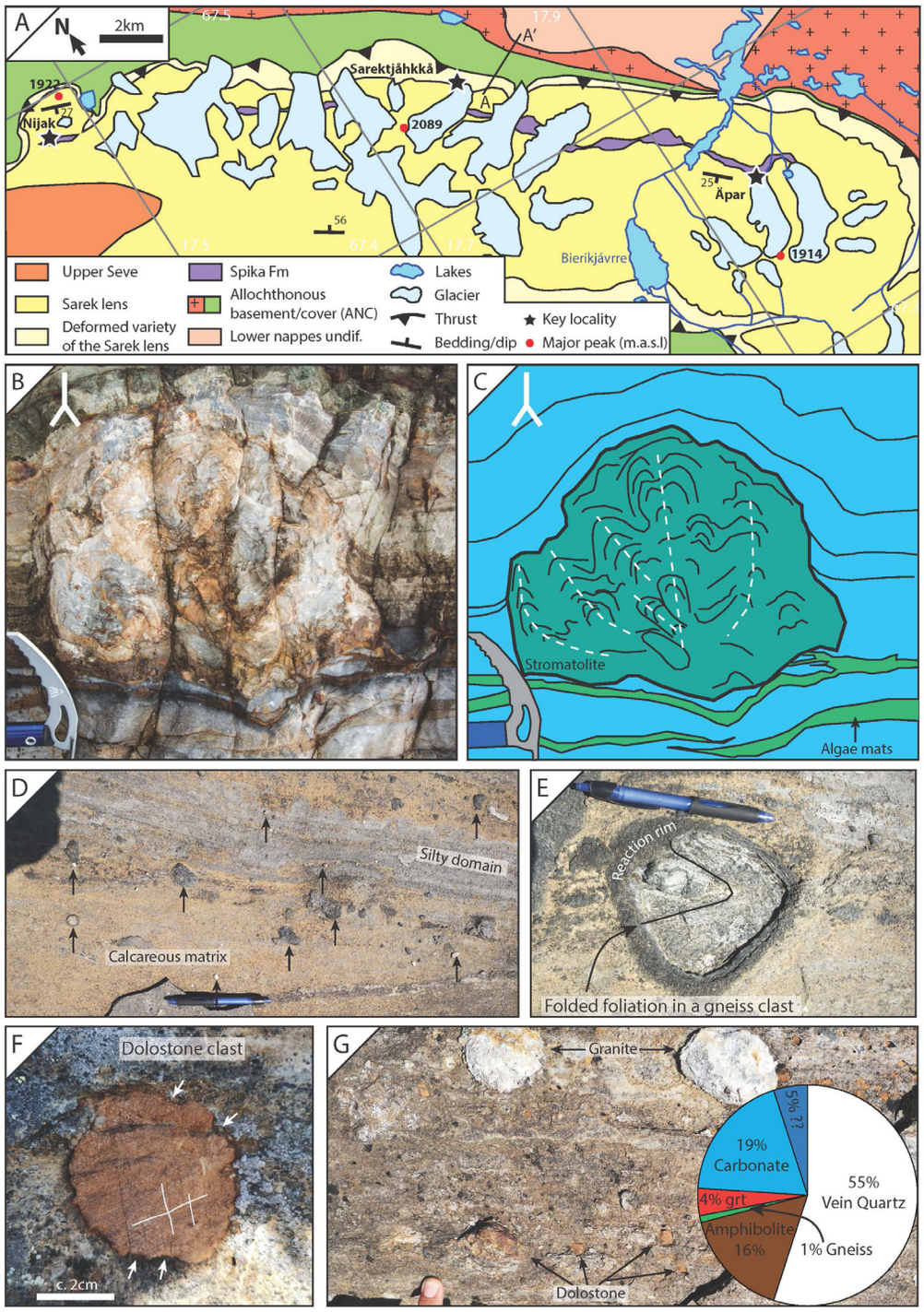

Figure 3. Map of northern Sarek and field observations of the stromatolites and the diamictite. (A) Geological map of northern Sarek modified from Svenningsen (1994a). Black stars with white rim indicate important localities referred to in the text. (B) Photograph of the columnar stromatolite found in the Äpar area in Sarek. Ice axe head for scale, front blade is c. 15 cm long. Note that the photograph is tilted clockwise by 90°. (C) Interpretation of the photograph in B. Green domains indicate growth structures. White dashed lines indicate ramifications. Note that they are oblique to the paleo-vertical. Note also onlap of carbonate to the side and the draping of the sedimentary layering over the top of the stromatolite. (D) Photograph of the diamictite matrix and clasts (highlighted by black arrows). Note the silty domain in the top half of the picture. Bedding is at low angle to the exposed section, which makes the silty domain appear thicker than it is. (E) Photograph displays a granitic gneiss clast in the diamictite with a folded foliation. Note the dark reaction rim towards the matrix. (F) Photograph of a dolostone clast from the diamictite. White lines highlight the characteristic criss-cross weathering pattern of dolostone. White arrows indicate grooves in the carbonate clast (G) Photograph of granite and dolostone clasts in the diamictite. Pie-chart shows distribution of clast lithologies. Note that only 19% of the clasts are sedimentary. Finger for scale in lower-left part of the photograph.

Observations from the Mihka, Skarjá and Akkajaure nappes at Sarek

The lower contact of the mega-boudin in Sarek is well exposed in the Sarektjåhkkå locality (Fig. 3A), and shows an almost continuous profile from the well-preserved core of the mega-boudin to the underlying Akkajaure NC. At this locality, the sedimentary succession and mafic dykes belonging to the Seve NC become progressively more overprinted by the Scandian deformation down section (Fig. 4C). In the core of the mega-boudin, the discordant relationship between the dykes and the sedimentary rocks can be discerned (Fig. 4B). Farther down section, the primary discordant contact relationship is lost and the developed foliation is parallel to the mafic layers (Fig. 4C). The metamorphic overprint increases down section and away from the core of the mega-boudin, and all primary textures are overprinted by a penetrative amphibolitisation, locally carrying garnet. The host rock varies from a marble to a quartz- and feldspar-rich metasediment. This deformed and metamorphosed unit is classically interpreted to be the Mihka unit (e.g., Andréasson et al, 1986). At a certain level in the lithostratigraphy, but not exposed, is a tectonic break where the garnets disappear. Below this contact, the Skárjá unit is present and the lithologies are dominated by feldspar-rich schist and metasandstone with some preserved feldspar porphyroclasts (Fig. 4D). Boudins of metadolerite are also common (Fig. 4D). Some of the boudins preserve a primary magmatic texture in the centre of the boudins. The asymmetry of both the boudins and the porphyroclasts suggests top-to-the-east kinematics (Fig. 4D). Towards the lower part of the Skárjá unit, some intervals are rich in quartz pebbles (generally within some few metres of the contact, Fig. 4E inset). The contact to the underlying Akkajaure orthogneiss is strained and contains several lenses of the underlying orthogneiss within the Skárjá unit. At the Sarektjåhkka locality, the Akkajaure orthogneiss has a mineral assemblage consisting of plagioclase + quartz + biotite + muscovite + titanite + epidote. Magmatic textures are rudimentary preserved in lenses devoid of strain (Fig. 4F). Domains that have accommodated more strain commonly show evidence for mylonitisation and/or cataclasis (Fig. 4F). Locally, pockets and veins of dark, very fine-grained material intrude into the gneiss (Fig. 4G). These pockets, with their sharp tapered offshoots, resemble pseudotachylite veins. Metadoleritic boudins, with primary magmatic textures locally preserved in their cores, are common. A top-west shear fabric (Fig. 4H) is locally discernible in the Akkajaure orthogneiss. Towards the contact with the overlying Skárjá unit, however, this fabric becomes progressively more overprinted by a top-east shear fabric. Close to the contact, east-verging folds refold all previous fabrics (Fig. 4E).

Results of the U–Pb geochronology

Sample localities and isotopic ratios and their corresponding ages can be found in the Electronic Supplements 2 & 3 (detrital zircon samples and sample HJK_2026, respectively). Analytical methods can be found in Electronic Supplement 4.

Detrital zircons

In order to investigate the maximum depositional age, sandstone samples were collected from all the five key areas with dyked Neoproterozoic sedimentary rocks presented in this contribution. U–Pb analyses of the detrital zircon grains were conducted using a LA-ICP-MS at the department of Geosciences at University of Oslo. Age probability diagrams (Kernel Density Estimates, KDE) were produced using the online software IsoplotR using 206Pb/238U age for ages younger than 1100 and 207Pb/206Pb ages for those older than 1100 Ma (Vermeesch, 2018). Likeness tests were constructed using the open source R-script “detzrcr” (Kristoffersen et al., 2016; Andersen et al., 2018). All presented analyses are less than ± 10% discordant and all uncertainties are 1σ (Fig. 5A).

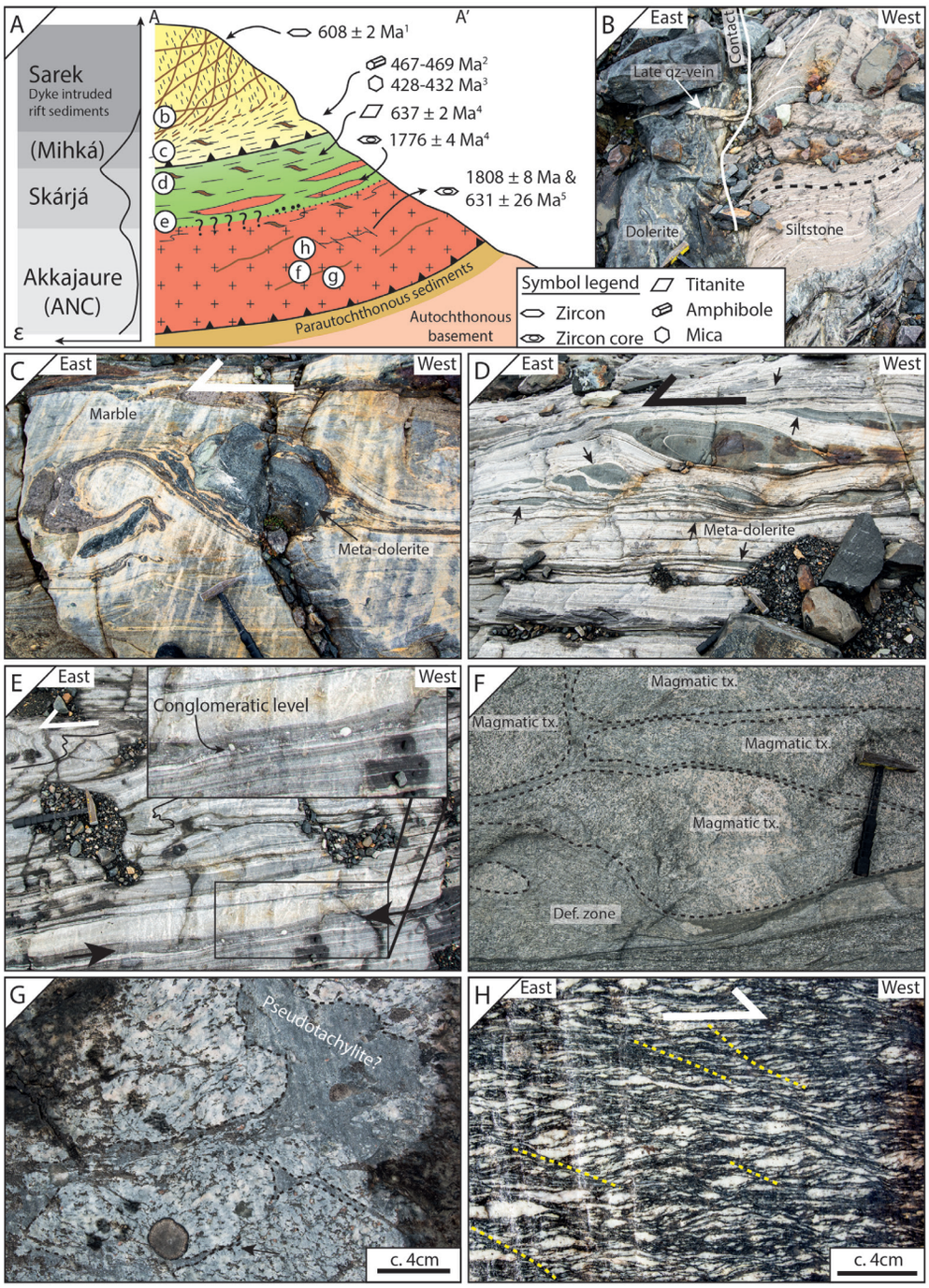

Figure 4. Photographs separated by c. 50 m of vertical stratigraphy. (A) Schematic diagram displaying the tectono-stratigraphy revealed at Sarektjåhkkå. A and A' indicate profile location from Fig. 3. Circles with letters indicate locations of the photographs shown below. Ages presented to the right of the sketch are from 1) Svenningsen, 2001, 2) Dallmeyer et al., 1991, 3) Svenningsen 2000, 4) Rehnström et al., 2002, 5) this study. (B) Discordant relationship between the bedding in a siltstone and a dolerite dyke. The siltstone shows some deformation possibly related to the emplacement of the dyke (see, e.g., Kjøll et al., 2019b). (C) A dolerite emplaced in a marble has been completely transposed and deformed into a delta-clast indicating top-east deformation. (D) Strongly deformed Skárjá unit with asymmetric mafic boudins that suggest top- East kinematics. Black arrows point to metadoleritic layers and boudins. (E) Photograph from close to the contact with the underlying Akkajaure orthogneiss showing horizons of monomict quartz conglomerate (black arrows), and asymmetric folds that indicate top-east kinematics. Inset shows an enlargement of the conglomeratic horizon. (F) Photograph of heterogeneously deformed orthogneiss that displays thin, discrete, proto-mylonitic shear zones highlighted by the black dashed lines. A magmatic texture (tx) is observed in the low-strain domains, delineated by the shear zones. (G) Pocket of very fine-grained, dark material, rich in clasts of the host rock, highlighted by the black dashed lines. Black arrow shows what appears to be an injection vein. (H) A top-west extensional crenulation cleavage is locally preserved in the orthogneiss. Yellow dashed lines indicate shear bands.

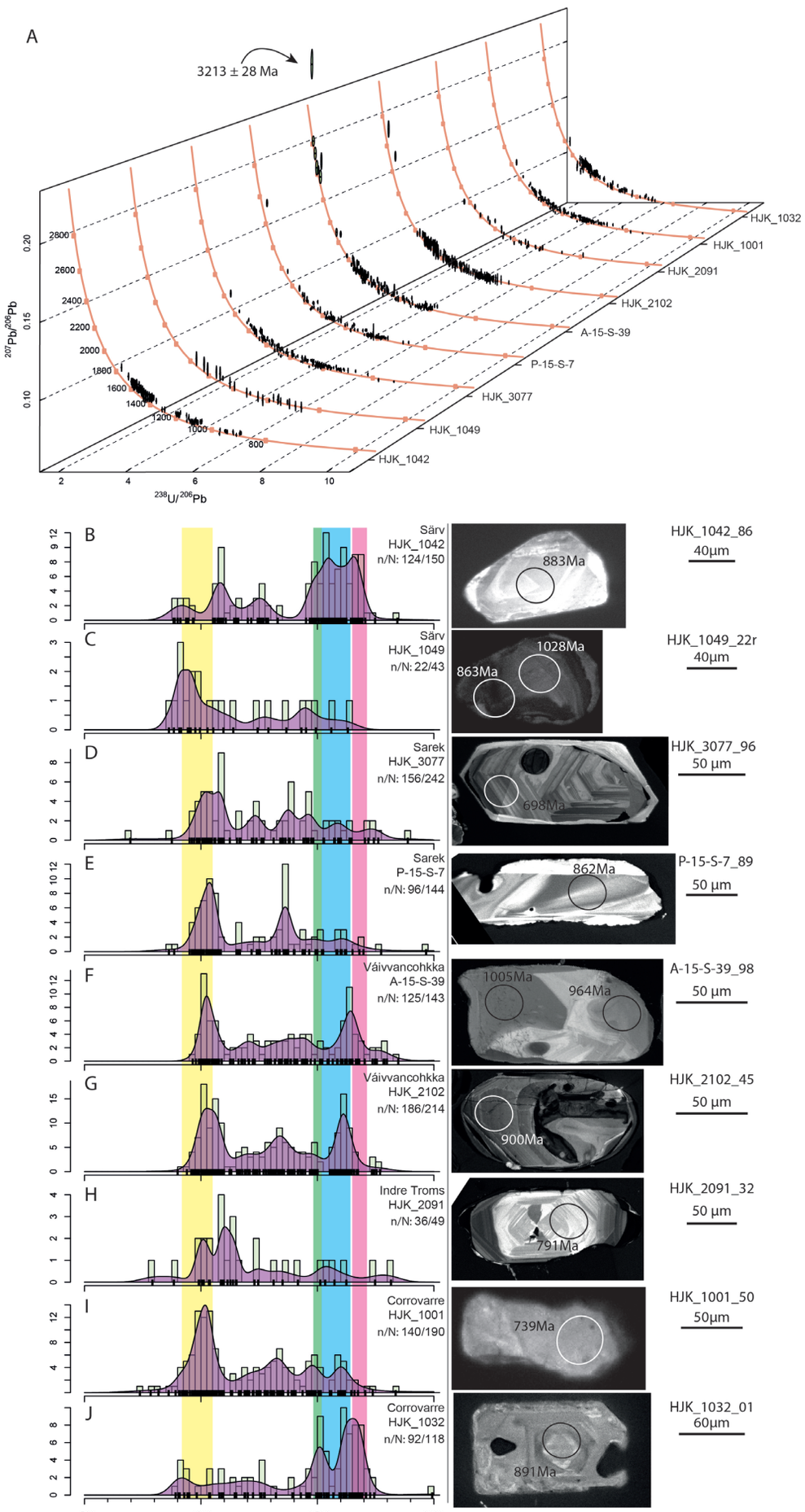

Figure 5. Detrital zircon analyses. (A) Compiled Terra Wasserburg Concordia diagrams that show all the data that are less than ± 10% discordant. Sample numbers are given to the right of the curve. (B–J) Combined age frequency (Kernel Density Estimate, KDE) and histograms for the less than ± 10 % discordant zircon analyses, using the free, open source "R" based software IsoplotR (Vermeesch, 2018). Ages younger than 1100 Ma are reported as $^{206}Pb/^{238}U$, whereas ages older than 1100 Ma are reported as $^{207}Pb/^{206}Pb$. NB: To better show the distribution of the majority of the data the histograms have been cut off at 2 Ga. See text and Electronic supplementary data for the analyses older than 2 Ga. Histogram bin width is 25 and KDE band width is 25. n/N indicate number of analyses less than 10 % discordant versus total number of analyses. Vertical coloured stripes: Yellow: Sveconorwegian (920-1050 Ma, Bingen et al., 2008; Bingen & Solli, 2009), Green: Telemarkian (1480-1520 Ma, Bingen, 2008), Blue: Gothian (1520-1640 Ma, Åhäll & Connelly, 2008), Magenta: Transscandinavian Igneous Belt (1650-1710 Ma, Larson & Berglund, 1992; Gorbatschev, 2004).To the right of the KDE are the Cathodoluminescence images of the youngest zircon of the sample. Circles indicate location of analysed spot with $^{238}U/^{206}Pb$ age.

Särv

Two samples were collected from Särv and both are from the Lunndörsfjällen Fm, which is the oldest formation in the Tossåsfjället Basin (Figs. 1 & 2).

Sample HJK_1042 is a medium-grained, white, quartzitic sandstone with some feldspar and minor biotite. The zircon grains are sub-rounded to prismatic and generally show a clearly developed oscillatory zonation, with some metamorphic resorption and growth. Of the total 150 analyses, 124 were less than ± 10% discordant. The youngest zircon of this sample has a $^{206}Pb/^{238}U$ age of 883 ± 7 Ma and has a strong CL signature where a magmatic zonation can be discerned (Fig. 5B). It is accompanied by two more grains of similar ages of 887 ± 8 Ma and 888 ± 7 Ma (- 7.2, 7.4 and - 5.3% discordant), respectively. Their weighted mean $^{206}Pb/^{238}U$ age of all the grains is 885.9 ± 4.1 Ma (MSWD = 0.56). In the detrital age distribution, three main peaks can be recognised at around 900, 1150 and a wide maximum at 1400 to 1500 Ma, the latter of which is the largest maximum (Fig. 5B). The oldest zircon has a $^{207}Pb/^{206}Pb$ age of 1843 ± 16 Ma.

The second sample, HJK_1049, is from the same formation and of similar composition as the sample described above. The zircon grains are rounded to prismatic and show some oscillatory zonation and some diffuse domains with lobate boundaries. The sample contained a total of 43 zircon grains and only 22 of the analyses were less than ± 10% discordant (Fig. 5C). Because of the low number of zircon grains, no statistical significance can be attributed to the distribution of ages (e.g., Andersen, 2005). The analysis of the youngest detrital zircon is concordant (- 0.4) and yielded an age that is similar to the sample described above with a $^{206}Pb/^{238}U$ age of 863 ± 18 Ma. It has a dark CL signature without a clear magmatic zonation (Fig. 5C). The youngest group of three zircons has a weighted mean $^{206}Pb/^{238}U$ age of 901 ± 21 Ma (MSWD = 0.75). The oldest analysed zircon has a $^{207}Pb/^{206}Pb$ age of 1631 ± 36 Ma.

Sarek

Two samples were analysed from the Äpar Formation in the Sarek area (Figs. 1 & 2). HJK_3077 was collected directly above the Nijak Fm. It is a medium- to coarse-grained quartzite, with minor micaceous material, feldspar and sulphides. The zircon grains have low aspect ratios generally less than 2. They are clear and prismatic and relatively large, commonly measuring >100 µm along their long axis. Most of the grains are euhedral and show very little rounding. In cathodoluminescence (CL), the zircons show a thin, bright rim of a few tens of µm thickness, surrounding rounded zircon grains (Fig. 5D), generally with a complex oscillatory zonation and varying CL intensities. 156 out of 242 analyses were less than ± 10% discordant. The youngest concordant (0.0%) analysis yielded a $^{206}Pb/^{238}U$ age of 698 ± 15 Ma. This zircon had a small round core with dark CL signature, whereas the rest of the grain has a well-developed oscillatory magmatic zonation, with a thin rim (Fig. 5D). The second youngest grain is 875 ± 13 Ma (- 7.7% discordant) and the youngest group of three overlapping zircon analyses has a $^{206}Pb/^{238}Pb$ weighted mean age of 963 ± 22 Ma (MSWD = 0.20). The age distribution of the sample is relatively wide with three maxima where the largest maximum is c. 1050 Ma. The other two maxima plot at c. 1300 Ma and 1450 Ma (Fig. 5D). Five analyses show a spread from c. 1650 to1810 Ma and one analysis is Archaean with a $^{207}Pb/^{206}Pb$ age of 2671 ± 23 Ma.

Sample P-15-S-7 is a medium- to fine-grained meta-arkosic sandstone with some mica-rich horizons. The zircons are mostly clear, with low aspect ratios that display little rounding. CL reveals that the grains have a thin, narrow rim with bright CL intensity. The cores generally have a darker CL signature and display a complex zonation commonly with multiple absorption-growth stages. 96 out of 144 analyses were less than ± 10% discordant. The youngest near-concordant (- 6.3%) zircon has a $^{206}Pb/^{238}U$ age of 862 ± 9 Ma and a bright CL signature with some diffuse zoning. The second youngest near-concordant

(- 3.6%) zircon is 885 ± 16 Ma. The three youngest zircon grains have a weighted average $^{206}Pb/^{238}U$ age of 959 ± 11 Ma (MSWD = 0.82). In this sample, the age distribution is dominated by two peaks, the largest is c. 1050 Ma and the other plots at c. 1300 Ma (Fig. 5E). One Archaean analysis yielded a 207Pb/206Pb ages at 2557 ± 11 Ma.

Váivvancohkka

Two samples were collected at Váivvancohkka from the upper part of the sandstone-siltstone unit (Figs. 1 & 2). A-15-S-39 is a silty fine-grained metasandstone (arkose-greywacke) rich in sulphides. The zircon grains are relatively round and small, measuring c. 20–50 µm. CL reveals that most grains have a complex oscillatory zonation locally with core-rim relations and locally with narrow rims with a bright CL signature. 125 out of 143 analyses were less than ± 10% discordant. The youngest zircon has a $^{206}Pb/^{238}U$ age of 964 ± 17 Ma, but this age is relatively discordant (- 9.9). The youngest near-concordant (- 0,7) zircon in the sample has a $^{206}Pb/^{238}U$ age of 1001 ± 20 Ma. The youngest group of zircons have a weighted average $^{207}Pb/^{206}Pb$ age of 1001 ± 15 Ma (MSWD = 0.13). The youngest zircon has an oscillatory zoned core with an irregular diffuse zonation at the tip, where the young age was measured (Fig. 5F). The zircon age distribution shows two peaks, one major that corresponds to c. 1050 Ma and two wide peaks at 1200–1400 Ma and 1550–1750 Ma (Fig. 5F). This sample also contained several Archaean grains, the oldest of which has a $^{207}Pb/^{206}Pb$ age of 3213 ± 28 Ma.

HJK_2102 is a fine- to medium-grained arkosic metasandstone sprinkled with white mica grains. The zircon grains are relatively euhedral and large, measuring generally ≥100 µm along the long axis. The aspect ratio of the zircon grains is usually relatively large and ranges from c. 2 to5. In CL, small cores are revealed that are overgrown by rims with oscillatory zoning. Out of a total of 214 analyses 186 were less than ± 10% discordant. The youngest zircon has a $^{206}Pb/^{238}U$ age of 900 ± 12 Ma and is - 3.2% discordant. The CL signature reveals that it has a large core with diffuse zonation, with an oscillatory zoned over-growth where the analysis was taken (Fig. 5G). The youngest group consists of three grains and has a weighted average $^{206}Pb/^{238}U$ age of 962 ± 9 Ma (MSWD = 0.28). Three peaks can be recognised from the age probability distribution function (Fig. 5G). The largest peak is at c. 1000 Ma. The second peak is at 1300 Ma and a double, partly conjoined peak at c. 1500 and 1600 Ma. Two out of the analysed zircons were Archaean and have $^{207}Pb/^{206}Pb$ ages of 2524 ± 16 and 2719 ± 22 Ma.

Indre Troms

One sample was analysed from Indre Troms, HJK_2091 (Figs. 1 & 2). The sample is of a medium-grained meta-arkose, rich in sulphides and mica. Only 50 zircon grains were recovered from this sample. These grains are sub-rounded and their CL signature generally shows complex oscillatory zonation, locally with resorption and neo-growth features. Out of 49 analyses, 36 were less than ± 10% discordant. The youngest near-concordant (- 7.5%) zircon has a $^{206}Pb/^{238}U$ age of 791 ± 15 Ma. The zircon displays a bright CL signature and beautiful sector oscillatory zonation (Fig. 5H). The youngest group of three zircon grains has an weighted mean $^{206}Pb/^{238}U$ age of 994 ± 23 Ma (MSWD = 0.027). The oldest zircon from this sample has a $^{207}Pb/^{206}Pb$ age of 1816 ± 14 Ma.

Corrovarre

Two samples have been collected from Corrovarre (Figs. 1 & 2), one from the northern part, HJK_1001, and one from the southern part, HJK_1032, of the tectonic lens. Both samples are from the Loddevággi Fm, but HJK_1001 is from lower down in the formation than HJK_1032 (Fig. 2). Sample HJK_1001 is a medium-grained, white, arkosic metasandstone with subordinate white mica and biotite. The zircon grains in HJK_1001 are generally rounded with a few prismatic grains. They are generally less than 100 µm and show oscillatory zoning. Older, small cores are commonly present. A total of 140 analyses out

of 190 were within ± 10% discordant. The two youngest zircon grains are 739 ± 8 Ma, 784 ± 23 at 2.7 and 3.5% discordance, respectively. The youngest grain has a homogeneous CL signature (Fig. 5I). The youngest overlapping group of three analyses has a 206Pb/238U weighted mean age of 903 ± 23 Ma (MSWD = 1.3). The data show a wide distribution with a clear peak around 1000 Ma and two smaller peaks at c. 1300 and 1400 Ma (Fig. 5I). No Archaean zircon grains were analysed and the oldest <10% discordant grain had a $^{207}Pb/^{206}Pb$ age of 2024 ± 14 Ma.

Sample HJK_1032 is a medium-grained, grey, arkosic metasandstone with some scattered white mica. The zircon grains are sub-rounded to prismatic. They are generally between 50–200 µm long and show oscillatory zoning and some metamorphic zonation. Out of 118 analyses, 92 are less than ± 10% discordant. The youngest zircon of this sample is 891 ± 10 Ma (- 1.6% discordant). This youngest zircon is euhedral and displays magmatic zonation (Fig. 5J). The youngest overlapping zircon grains have a 206Pb/238Pb weighted mean age of 906 ± 10 Ma (MSWD = 0.052). This sample has a relatively large population of 8 grains out of 94 that gave ages ranging from 900–1000 Ma. The age distribution of the sample has its largest maximum at 1500–1700 Ma (Fig. 5J). The oldest grain has a $^{206}Pb/^{207}Pb$ age of 1993 ± 22 Ma.

Age dating of the ANC at the contact to Skárjá

Analytical data for sample HJK_2026 can be found in Electronic Supplement 3 and analytical methods, which were the same as for the detrital zircon analysis, can be found in Electronic Supplement 4. Ages and intercept ages were calculated using the open source software 'IsoplotR' (Vermeesch, 2018).

Sample HJK_2026 is from the Akkajaure orthogneiss and display a top-west extensional crenulation cleavage (ECC) shear fabric (Fig. 4A, H, see section 4.3 for a mineralogical description of the orthogneiss). The recovered zircon population of sample HJK_2026 is relatively anhedral and homogenous with a milky, light brown appearance (Fig. 6A top right inset). Using a Cathodoluminescence (CL) detector mounted to a Hitachi SU6500 SEM, it became evident that the zircons had a magmatic zonation with relatively low CL signal. The magmatic zonation is locally replaced by thin rims and healed fractures of

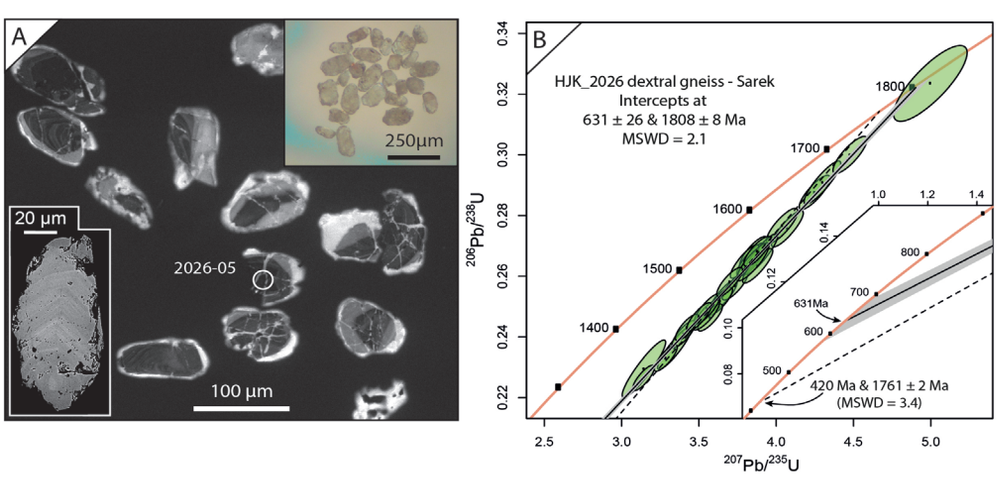

Figure 6. Results from the zircon dating of the Akkajaure orthogneiss with a top-west fabric. (A) Cathodoluminescence images of zircon grains from sample HJK_2026. Note growth zonation overprinted by numerous fractures with a brighter signature. Inset in top-right corner shows photomicrograph from optical microscope and inset in lower-left corner show a high-contrast backscatter electron image that reveals magmatic zonation. (B) Concordia diagram of all the spot analyses from sample HJK_2026. The solid line is calculated from the data, with no anchors, and provides the upper and lower intercept discussed in the text. The grey shading indicates the error. Inset to lower right shows the lower intercept of the Discordia line. The dashed line was calculated when the lower intercept is anchored to 420 Ma. Note the somewhat larger MSWD.

a zircon with a stronger CL signal (Fig. 6A). The zircon grains were mounted in epoxy and polished for LA-ICP-MS analysis according to the method described in Electronic Supplement 4. The data are linearly discordant, with one near-concordant analysis (- 1.6% discordant) with a $^{207}Pb/^{206}Pb$ age of 1833 ± 20 Ma (Fig. 6B). Fitting a Discordia model-2 line through the data yields an upper intercept age of 1808 ± 8 Ma and a lower intercept of 631 ± 26 Ma with a MSWD of 2.1 (Fig. 6B).

Discussion

Rift-related extensional deformation recorded in the Akkajaure NC

The zircon analyses from sample HJK_2026 all plot along a single, straight regression line, with a MSWD of 2.1 (Fig. 6). This indicates a closed system recording lead loss from originally magmatic grains during one tectonothermal event. The characteristic healed fracture pattern, observed as a bright CL signal in the zircon grains, indicates brittle fracturing and rapid precipitation and sealing due to, e.g., a drop in fluid pressure during the fracturing, which is often observed in other more common rock-forming minerals as well (e.g., Rimsa et al., 2007; Kjøll et al., 2015). Austrheim & Corfu (2009) observed similar zircon microtextures, as described above, in rocks subjected to very high strain rates achieved during formation of ultracataclasites and pseudotachylites. At the Sarektjåhkkå locality, veins with extremely fine-grained material, resembling pseudotachylite (Fig. 4G), have been observed in close proximity to the areas that show a top-west shear fabric, which indicates that the fracturing of the zircons may have formed under a co-seismic event. The deformed orthogneiss that preserves the top-west shear bands was deformed under fluid-rich greenschist-facies conditions, as evidenced by neo-growth of hydrous minerals such as muscovite, epidote and biotite. Several studies have suggested that zirconium can be mobile at temperatures as low as 250–350°C under favourable chemical conditions, and the fracture-fill could thus have formed under the conditions recorded in the shear zone (Dempster et al., 2004; Rasmussen, 2005).

The upper-intercept age of 1808 ± 8 Ma is interpreted to represent the protolith age of the orthogneiss, as it is similar to previously published protolith ages from the same unit (e.g., 1800 ± 2 and 1795 ± 4 Ma in Rehnström & Corfu, (2004) and 1806 ± 15 Ma in Kirkland et al., 2011). By fitting a line through the data, without imposing any interpretations, i.e., anchoring the lower intercept to a specific time, the data show a lower-intercept age of 631 ± 26 Ma. This lower-intercept age is interpreted to reflect the top-West shearing event as the sample shows no evidence of structures associated with any other major tectonothermal event. Moreover, the lower-intercept age overlaps within error with the much more precise ID-TIMS age of a 637 ± 3 Ma metamorphic titanite from Rehnström et al. (2002), corroborating the notion of a tectonothermal event at this time. As the titanite age presented by Rehnström et al., (2002) did not have any structural constraints, the authors therefore could not confidently associate the age with any specific tectonic event and both terrane accretion and extension were suggested. The overlapping age presented here, however, comes from a top-west orthogneiss, the data of which indicate just a single episode of Pb loss, and is therefore likely to represent the deformation event. It is therefore proposed that because of 1) the overlap in ages between the lower intercept presented here (631 ± 26 Ma) and what is presented in Rehnström et al. (2002, 637 ± 2 Ma), 2) the tectono-stratigraphic position of the Skárja unit below the Sarek lens, and 3) the assumed tectonic setting of Baltica and Laurentia at this time, the age, and therefore the fabric recording top-west kinematics, corresponds to an extensional event. This implies that the crust between Baltica and Laurentia was attenuating and thinning at c. 637 Ma, which was presumably associated with a surface depression

and hence providing accommodation space for the sedimentary successions, now preserved within the nappes of the Scandinavian Caledonides. Whether this records the onset of rifting or some event in the middle of the rifting history cannot be constrained, but it indicates that the middle crust was undergoing both co-seismic and ductile deformation at around 637 Ma.

Across-basin correlation

There are several similarities between the individual Neoproterozoic basins that have been preserved in the dyke-intruded Särv and Seve NCs in the Scandinavian Caledonides. Some of these similarities are summed up below.

Lithostratigraphy

All the basins discussed contain formations that are dominated by dolostone intercalated with calc-silicate layers (Fig. 2). In Särv, Sarek and Indre Troms these carbonate formations have been described as locally containing evaporite deposits, because of the presence of Cl-rich scapolite formed during contact metamorphism, chert nodules and magnesite deposits (Kumpulainen, 1980; Svenningsen, 1994b; Kjøll et al., 2019a). The depositional environment for these rocks has been interpreted to be sabkha and lagoonal-type environments, typical for tropical to sub-tropical latitudes (e.g., Kumpulainen & Greiling, 2011; Svenningsen, 1994b).

The top of the Spika Fm. in Sarek contains stromatolitic carbonates, which were discovered during this study. These columnar stromatolites are similar to *Eleonora laponica,* which is found in the Porsanger dolomite in Finnmark (cf., Grasdal Fm., Fig. 1, Bertrand-Sarfati & Siedlecka, 1980; Nystuen et al., 2008) and in the Eleonore Bay Supergroup in eastern Greenland (e.g., Caby & Bertrand-Sarfati, 1976; Halverson et al., 2004; Sønderholm et al., 2008). The age of the stromatolites is suggested to be Late Riphean (i.e., 1400–800, Vidal, 1976) or Vendian (i.e., 650–542 Ma, Bertrand-Sarfati & Siedlecka, 1980). Because of the large age uncertainty for these stromatolites they cannot be used confidently to further constrain the time of deposition. They are, however, useful as they indicate the paleo-depositional environment and because they are reported to occur in a similar stratigraphic position in other circum-Iapetus basins.

Another possible lithostratigraphic marker are the diamictites. Their stratigraphic position in the heavily dyke-intruded Sarek and Särv areas are remarkably similar. The diamictites separate shallow-marine carbonates with traces of evaporites from thick packages of clastic sediments. The conglomerate described by Stølen (1994) from Indre Troms could also represent such a diamictite unit. Its stratigraphic position is similar to that in Sarek and Särv on top of dolostone and impure marbles with calc-silicate horizons and evaporite deposits. The description is unfortunately sparse and the outcrop can only be reached with climbing gear and experience. Similar stratigraphic relationships are also found in the Uppermost Allochthon in the Scandiavian Caledonides where diamictites are described from carbonate units (e.g., Melezhik et al., 2015). Based on correlation of $^{87}Sr/^{86}Sr$ and $\delta^{13}C$ isotope composition to global seawater curves, these particular units are interpreted to have been deposited in the Mid to Late Cryogenian on what would become the Laurentian margin after the c. 608 Ma break-up (Svenningsen, 2001; Melezhik et al., 2015; Kjøll et al., 2019a).

The characteristic intercalated dolomite and calc-silicate unit with stromatolites and diamictites could thus serve as a marker unit for inter-basinal correlation between the distal basins (Sarek, Váivvancohkka and Indre Troms).

Likeness of the detrital zircon age distributions

For the following discussion, the two samples HJK_1049 and HJK_2091 are omitted from the detrital zircon dataset, due to the low number of retrieved zircon grains. The age distribution of the rest of the detrital zircon record can be used to evaluate similarities between the individual samples and thereby similarities between the different basins. Two different methods are used here, the 'likeness test' and 'upper and lower quartile' plots. Table 1 displays the results of the 'Likeness test'. The likeness test investigates the percentage of 'sameness' between two unitised probability density plots (Satkoski et al., 2013). Several of the calculated values are close to or higher than the average likeness of 0.72 ± 0.06 expected from a set of c. 100 randomly selected zircon analyses from a single population (Satkoski et al., 2013). This method does not take into account the error of the individual analysis, and the age distributions therefore tend to be more unlike each other than if the error had been taken into account. The average number of analyses conducted per sample for this contribution is 131. The samples that are statistically indistinguishable are highlighted in bold. From the likeness data it becomes evident that the sample from Särv (HJK_1042) is relatively dissimilar to the samples from Sarek and Váivvancohkka as well as one sample from Corrovarre (HJK_1001, Tab. 2). Sample HJK_1032 from Corrovarre is, when using the likeness test, statistically indistinguishable from the sample from Särv (HJK_1042, Tab. 1). This similarity between the most distant samples is interesting and suggests that the basin detritus for these samples (HJK_1032 and HJK_1042) was sourced from an area with similar age distributions, but different from the one in Sarek, Váivvancohkka and Indre Troms. All four samples from the central part of the study area, i.e., Sarek and Váivvancohkka, are statistically indistinguishable (Tab. 1). One sample from Corrovarre (HJK_1001) is also similar to those from the central areas, except for sample A-15-S-39 from Váivvancohkka, since the Corrovarre sample has a lower 1600 Ma peak (Fig. 7).

Another way of comparing the populations of the detrital zircon record is by an upper/lower quartile plot, which transforms the age distribution into one point based on the median of the upper quartile (75%) and the median age of the lower quartile (25%, Fig. 7, Andersen et al., 2018). In this scheme, a homogeneous population of zircon grains from, e.g., a tuff layer would plot on the 1:1 line (Andersen et al., 2018). When plotting the cumulative distribution of the detrital zircon data we see that the shapes of the age distribution of the samples are relatively similar. Samples 1042 and 1032 are slightly different with a few zircon grains in the range 1200–1400 Ma (Fig. 7A). When plotting the upper quartile and lower quartiles against each other it becomes evident that there is a larger spread in the upper quartile than the lower quartile and that samples 1032 and A-15-S-39 are relatively distant, compared with the rest of the samples (Fig. 7B). Sample A-15-S-39 plots as an outlier on the upper quartile but it is, however, similar to the other samples on the lower quartile (Fig. 7B). A mixing line can be drawn between the samples that indicates that the 1050 Ma and 1550 Ma sources contribute considerably to the age spectra.

Table 1. Results of 1D likeness test (Satkoski et al., 2013). The table compares the Särv, Sarek, Váivvancohkka, Indre Troms and Corrovarre samples from south to north. Bold areas have statistically indistinguishable detrital zircon age populations.

			South → North						
			Särv	Sarek	Sarek	Váivan.	Váivan.	Corro	Corro
			1042	3077	P–15–S–7	A–15–S–39	2102	1001	1032
South → North	Särv	1042	–	0.644	0.543	0.541	0.649	0.581	**0.834**
	Sarek	3077		–	**0.8**	**0.754**	**0.887**	**0.849**	0.621
	Sarek	P–15–S–7			–	**0.732**	**0.819**	**0.842**	0.542
	Váivan.	A–15–S–39				–	**0.796**	0.699	0.605
	Váivan.	2102					–	**0.818**	0.643
	Corro	1001						–	0.572
	Corro	1032							–

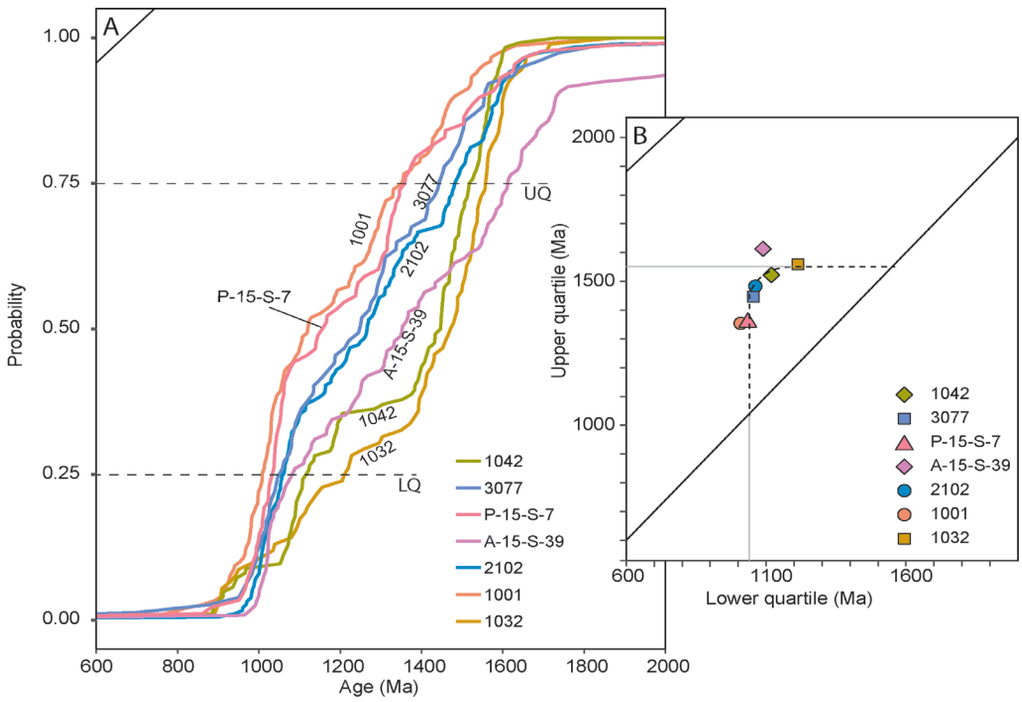

Figure 7. Cumulative age distribution and upper quartile - lower quartile diagram. (A) Cumulative age distribution shows all the samples and their respective upper and lower quartile values (UQ and LQ, respectively, marked by dashed black line). (B) UQ and LQ are plotted against each other. A mixing line shows that the main population can be described as a mix of a 1050 and 1550 age component.

The results from the likeness test and the upper vs. lower quartile plot suggest that the detritus in the central areas, i.e., Sarek and Váivvancohkka and also partly Corrovarre, most likely received detritus from source rocks of similar ages, since their detrital zircon age distributions are statistically indistinguishable, whereas Särv may have received detritus from a different or additional source.

Tectonometamorphic development

Further indications that corroborate a correlation between the exposed basins are the tectonometamorphic histories of the different areas. First, the mafic dyke swarm has been dated at Särv, Sarek and Corrovarre, and the ages are close to fall within error of each other at 596 ± 10, 608 ± 1 and 605 ± 1.8 (Svenningsen, 2001; Kumpulainen et al., 2016; Kjøll et al., 2019a). Second, Kjøll et al. (2019a) estimated a similar crystallisation depth for the mafic dykes at 2.5–4.5 kbar for all three areas. It can thus be suggested that the dyke swarms that intruded the sedimentary basin successions are part of the same event, and that they roughly correspond to the same depth. Third, the investigated areas form an almost continuous line of exposures from Sarek through Váivvancohkka and Indre Troms to Corrovarre (Fig. 1). Fourth, in the central areas in Sarek, Váivvancohkka and Indre Troms the contact-metamorphic overprint in the mega-boudins, as well as the metamorphic overprint in the surrounding Seve NC is similar. This suggests that these central areas experienced similar tectonometamorphic histories, and that they were connected, or at least in similar palaeogeographic positions along the pre-Caledonian Iapetus margin.

Corrovarre, in Troms, northern Norway, is a small allochthonous tectonic sliver located between the Kalak NC and the Palaeozoic aged Reisa NC. The tectonic sliver, similar to the other areas, has a well-preserved core that is devoid of most of the Caledonian strain and thus provides a window into the Neoproterozoic history. The Corrovarre tectonic lens is generally considered to be the uppermost level

of the Kalak NC in this part of Troms (Zwaan & Van Roermund, 1990; Lindahl et al., 2005). Numerous studies have shown that the Kalak NC has a complex Neoproterozoic history with high-pressure and temperature events likely occurring during the period from c. 800 to580 Ma (e.g., Kirkland et al., 2006; Gasser et al., 2015). The Corrovarre lens, however, primarily records a high-temperature, low-pressure event (Zwaan & Van Roermund, 1990; Kjøll et al., 2019a) and is thus significantly different from the higher grade 'basement' rocks of the Kalak NC, and it is therefore unlikely that the two shared a common pre-Scandian tectonometamorphic history. To untangle the complex Neoproterozoic history of the Kalak NC and the Corrovarre lens, more targeted work is needed.

The data presented above indicate that there are great similarities between the discussed sedimentary basins, not only in the detrital age distributions, but also in their magmatic, sedimentary/lithological and tectonometamorphic records. It is therefore proposed that the similarities in the detrital zircon age distributions (Fig. 7, Tab. 1), stratigraphy of the sedimentary successions (Fig. 2) and the similarities of the early dyking (Kjøll et al., 2019a, b) suggest that the basin subsidence and sedimentation occurred during the same major plate-tectonic event for all the different basins.

Maximum depositional age for the sedimentary succession

As described above (section 6.2.3.), the entire stratigraphy of all the palaeobasinal domains preserved in the Särv and Seve NC, and Corrovarre were cut by the mafic dykes at c. 608–596 Ma, clearly showing that the deposition of all the sedimentary successions occurred before c. 608 Ma. A maximum age for the deposition is more challenging, however. No syn-tectonic magmatic products have been observed thus far within the sedimentary successions. Despite inherent problems in estimating the depositional history and provenance of sediments from clastic zircons (e.g., Andersen, 2005; Andersen et al., 2016), the youngest detrital zircon is the best choice to find an indication for the maximum depositional age. Baltica and Laurentia were, however, tectonically relatively quiet for most of the Late Tonian to Cryogenian, except for late- to post-orogenic Sveconorwegian intrusions (Bingen et al., 2008; Bingen & Solli, 2009), and extrusion of a flow-banded lava with rhyolitic-dacitic composition at 945 ± 35 Ma (Albrecht, 2000). In addition, there was the emplacement of a bimodal magmatic complex at c. 845 Ma, the emplacement of the Hunnedalen dyke swarm at 855 Ma and a number of tectono-metamorphic events recorded in the Kalak NC in northern Norway (e.g., Walderhaug et al., 1999; Paulsson & Andréasson, 2002; Kirkland et al., 2006; Corfu et al., 2007; Gasser et al., 2015).

The youngest analysed zircon from all the sedimentary successions presented here is a concordant age of 698 ± 15 Ma from an oscillatory-zoned detrital zircon from Sarek (Fig. 5C, Electronic Supplement 1). It is sampled from a sandstone deposited directly on top of the Nijak Fm diamictite (Fig. 2). One should be careful not to rely too much on a single grain analysis, although in this case, the analysis is concordant and done on a relatively large grain with clear magmatic zonation, reducing the likelihood that the young age is an artefact of post-crystallisation Pb loss. Furthermore, similarly aged zircon grains are also found in Corrovarre; 739 ± 8 Ma and from Indre Troms; 791 ± 15 Ma (Fig. 5H, G). It should be noted, however, that the 739 Ma zircon from Corrovarre has a homogenous CL signature, which could indicate some hydrothermal alteration of the zircon (Corfu et al., 2003). From previously published detrital zircon studies either from Särv or from the deformed part of the Seve NC, similarly young detrital zircons (700–800 Ma) are present in some of the analysed samples, but they are not common (Be'eri-Shlevin et al., 2011; Kirkland et al., 2011 Gee et al., 2014). In some of the samples presented here, intermediate detrital zircon ages between the youngest single zircon analysis and the youngest group analyses, are present (Fig. 8). These analyses are not overlapping in age and are therefore giving an artificially big gap between the youngest single grain analysis and the youngest group. It is therefore proposed that, with some caution, these youngest zircon analyses from each sample give an indication for the maximum depositional age of the sediments. If one accepts these detrital zircon ages as maximum depositio-

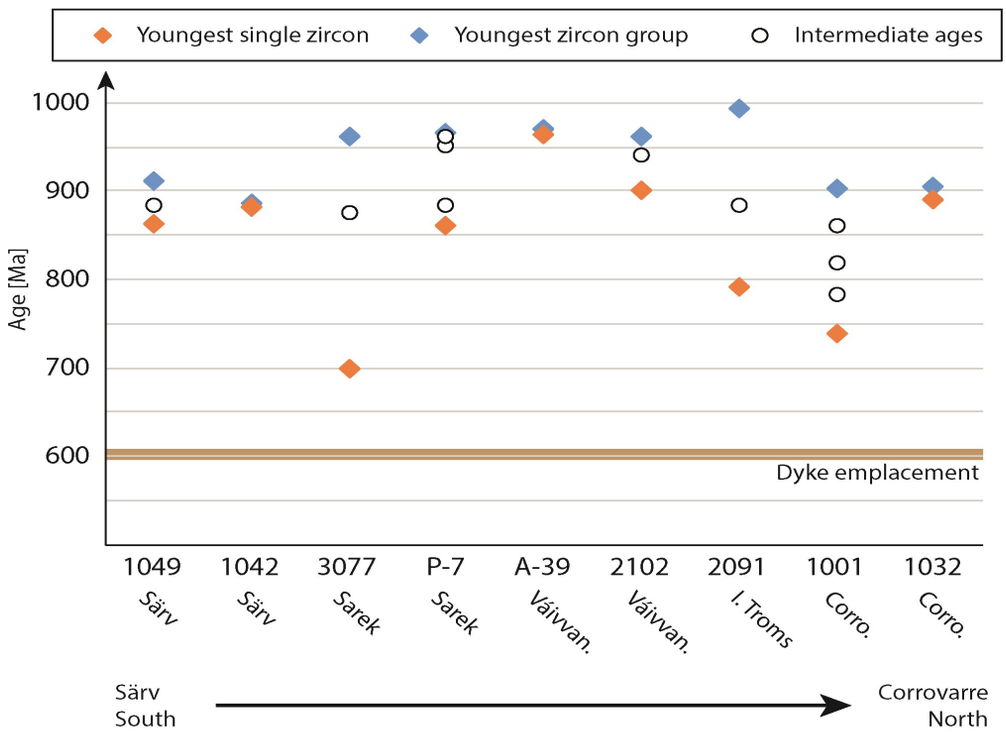

Figure 8. Diagram showing the youngest analysed detrital zircon from all samples presented in this study (orange), the youngest group from each sample (blue) and the intermediate ages (white circles with black rims), which do not have overlapping errors and are therefore not included in the youngest group of zircons. The brown line shows the age-range of dyke emplacement based on previously published U-Pb ages from the dyke complex (see references in text) and thus the minimum age of deposition.

nal ages for the basins, they bracket the age of deposition to c. 90 M.yr. for the Sarek area. Furthermore, the age may also provide an upper limit for the onset of rifting, as the detrital zircon sample was collected at the boundary between the shelf carbonates, directly below the diamictite, and the several kilometres-thick, siliciclastic Äpar Fm. in Sarek (Fig. 2). This transition marks a significant change in sedimentary influx and depositional environment, possibly reflecting the change from a slowly subsiding sag-basin with little sedimentary influx to a rapidly subsiding rift basin, with a large siliciclastic input, derived, e.g., from an uplifted rift flank.

A note on source region provenance

Gee et al. (2014), Ladenberger et al. (2014) and Be'eri-Shlevin et al. (2011) discussed the provenance of the sediments from the Särv- and southern part of the Seve NC. Because of the wide variety of magmatic and metamorphic ages and the lack of Archaean ages in the Särv detritus, they argued that the entire age spectra was sourced from the Fennoscandian Shield. Kirkland et al. (2011), on the other hand, argued that there is an overlap in magmatic and metamorphic ages from Laurentia and Baltica and that a distinction between the source areas is difficult to make. The challenges of deciphering Baltica vs. Laurentia derived detritus is also discussed in Slagstad & Kirkland (2017) who show that separating different terranes in the Scandinavian Caledonides using detrital zircons is impossible, because of the non-unique distribution of Precambrian rocks on Baltica and Laurentia. Furthermore, basing provenance studies solely on U–Pb and Lu–Hf detrital zircon signatures is insufficient to robustly confirm either a Baltican or a Laurentian affinity. Because of the aforementioned challenges, a provenance study will not be attempted using this dataset.

A glaciogenic origin of the Nijak Formation?

The conglomerates, as referred to by Stølen (1994) and Svenningsen (1994a), are matrix-supported, polymict diamictites (Fig. 3 and Electronic supplementary Fig. 1, See detailed description of the Nijak Fm. in section 4.2). Diamictites can be formed by glacial processes, glacial-influenced processes and non-glacial processes (e.g., Eyles & Januszczak, 2004; Le Heron & Vandyk, 2019). The non-glacial alternatives include terrestrial or marine debris flows, lahars, fault gouges, regolith formation and impact breccias (Eyles & Januszczak, 2004), some of which may be excluded directly for the Nijak Fm. based on several key observations; the Nijak Fm is polymict with some rounded clasts and a matrix that shows some indications of reworking by water. This excludes lahars (volcanic clasts), regolith formation (monomict), impact breccia (monomict and pseudotachylite) and fault breccia (clasts reflecting footwall and hanging wall lithologies) as being responsible for the formation of the Nijak diamictite. Debris flow, on the other hand, is a more likely formation mechanism. Debris flows from topographic highs formed by fault activity at rifted carbonate shelves are often invoked to explain the presence of carbonate clasts within diamictites (Eyles & Januszczak, 2004; Creveling et al., 2016). Such carbonate clasts are also present in the diamictite units described and referred to here but cannot explain the presence of the relatively high percentage of metamorphic clasts (at least 17%) and magmatic clasts (60%, Fig. 3G), i.e., basement-derived clasts, especially since the diamictite units are directly underlain by at least 800 metres in Sarek (Svenningsen, 1994a, b), and at least 4000 metres of shallow-water carbonates and clastic sediments in the Tossåsfjället Basin (Kumpulainen, 1980, 2011). Furthermore, most paleogeographic models infer a wide, pre-Caledonian, Iapetus margin based on, e.g., palinspastic reconstructions of the margin, Early Ordovician subduction-related metamorphism as well as observations of extensive carbonate platform sediments (Siedlecka et al., 2004; Nystuen et al., 2008; Pease et al., 2008; Andersen et al., 2012; Root & Corfu, 2012; Jakob et al., 2019). The presence of these extensive, shallow-marine, carbonate platforms directly underlying the diamictite formations suggests that the palaeo-slope presumably was gentle and would therefore complicate deposition of debris flows derived from a land area. Another way of introducing basement clasts would be to uplift the footwall of large faults. In the case of Sarek, such a fault would need a throw of more than 800 metres to expose the basement. There are, however, no indications for such major fault activity penetrating the sediments and presumably causing local rotations, erosion and redeposition, either in Sarek or in the Tossåsfjället basin. A debris-flow origin for the Nijak Fm. is therefore assumed to be less likely but cannot be completely ruled out.

For a diamictite to be considered as glaciogenic, deposited in an ice-contact environment, a number of key factors must be present. Eyles & Januszczak (2004) proposed the following factors: 1) Striated clasts, 2) Deposition on a striated and/or erosive pavement, 3) restrictive thickness, less than 100 m thick, 4) far-travelled clasts, 5) reworking and resedimentation due to meltwater release, and 6) rapid vertical and lateral facies changes due to topographic control during deposition. Kumpulainen & Greiling (2011) further argued for a large regional extent of diamictite formation and fixed regional stratigraphic position as criteria for a glaciogenic origin. Because of the challenging condition at the outcrop, regarding both metamorphic overprint and blocky outcrop, not all of these factors could be deduced. What is clear is that the Nijak Fm.: 1) contains a significant proportion of far-travelled basement clasts, 2) displays rapid lateral facies changes, 3) has a restricted thickness (5–10 m thick), 4) displays reworking/resedimentation in some parts of the unit, 5) has a fixed regional stratigraphic position (on top of a carbonate unit with evidence for evaporite deposits), and 6) some carbonate clasts have what appear to be striated surfaces (Fig. 3F). This last point is of course challenging to assess in 2D, but is, nevertheless a compelling observation, which could suggest a glaciogenic origin for the Nijak Fm.. A striated or erosional depositional surface, on the other hand, has not been observed below the Nijak Fm., due to the poor conditions at the actual outcrop.

A more detailed study of the clast geometries and stratigraphy would be useful for a more assertive conclusion of the depositional environment for the Nijak Formation. Based on the characteristics of the diamictite presented above, it is suggested that the Nijak Fm. may have been deposited either by direct glacial or glacial-influenced processes, such as a fluvioglacial or submarine glacial outwash deposit (e.g., Edwards, 1986). If the latter is true the secondary reworking must have been sufficiently short lived to have preserved the asperities on the surface of the dolostone clasts. An origin as a debris-flow deposit cannot be completely ruled out, but is deemed less likely.

The age of the diamictite cannot be confidently established, but since it is cut by dated mafic dykes in both the Tossåsfjellet and the Sarek basin, it must be older than 596 Ma and 608 Ma, respectively. This rules out the 580 Ma Gaskiers glaciation for these two diamictites (Bowring et al., 2003; Pu et al., 2016). In Sarek, the youngest detrital zircon, sampled from directly above the Nijak diamictite, is 698 Ma. Bearing in mind that there is a >2500 m-thick siliciclastic unit resting on top of the Nijak Fm., this suggests that the diamictite was deposited well before 698 Ma. If the deposition was associated with one of the major Neoproterozoic glaciations, this would favour the Marinoan glaciation that took place at c. 635 Ma (Hoffmann et al., 2004).

Conclusions

This paper presents new field observations as well as analytical data from well-preserved mega-boudins of dyke-intruded, sedimentary successions in the Särv and Seve NC in northern Sweden and Norway. The main conclusions from this study are:

1. The transition from the deposition of the Spika Fm. to the Äphár Fm. in Sarek marks a significant change in sedimentary influx and depositional environment, possibly reflecting the change from an early sag-basin to onset of rifting with rift-flank uplifts.

2. The Nijak Fm. is interpreted to have been deposited either directly by glacial processes or by some glacial-influenced processes. An origin as a debris-flow deposit cannot be ruled out, but is deemed less likely. The Nijak Fm. could possibly be related to one of the earliest major Neoproterozoic glaciations, i.e. the 635 Ma Marinoan glaciation or the 712 Ma Sturtian glaciation.

3. The first observation and description of a well-preserved unit of columnar stromatolites in the Seve NC is presented. The stromatolites appear to be *Eleonora laponica*, which is well known from other neoproterozoic, circum-Iapetus, carbonate deposits.

4. The youngest detrital zircon analysis from Sarek indicates that the sampled metasedimentary rock was deposited after c. 700 Ma, suggesting that the accumulation of the sedimentary succession is bracketed by c. 90 M.yr. by the youngest analysed detrital zircon and the emplacement of the mafic dyke swarm. A similar relationship is observed for Corrovarre, where the youngest detrital zircon is 739 Ma and the mafic dykes have been dated to 605 Ma.

5. Fractured and healed zircons found in an orthogneiss displaying a top-west, ECC fabric in the vicinity of fine-grained, dark veins resembling pseudotachylite veins suggest both ductile and frictional, co-seismic deformation.

6. LA-ICP-MS dating using U–Pb on zircon from the orthogneiss indicates that the middle crust between Baltica and Laurentia was deforming at c. 631 ± 26 Ma. This age is within error of the

previously published and more precise U–Pb titanite age of 637 ± 2 Ma (Rehnstöm et al., 2002), and could suggest that the crust was thinning and creating accommodation space in the basins above.

7. Similarities in the detrital zircon age distributions, youngest analysed detrital zircon group, the key units in the sedimentary stratigraphy and the geological similarities when it comes to dyking and metamorphism, suggest that the basin subsidence and sedimentation occurred during the same major plate-tectonic event.

Acknowledgements. Loic Labrousse is thanked for his help during fieldwork, both with understanding the geology, carrying samples and keeping us safe on the glacier! Johan Petter Nystuen, Lars Eivind Augland, Johannes Jakob and Torgeir B. Andersen are thanked for reading early versions of this manuscript and discussing the data. Marius Tevik Olsen, Magnus Kristoffersen, Gunnborg Bye Fjeld and Siri Simonsen are thanked for assistance with sample preparation and laser ablation analyses at the University of Oslo. D. P. Le Heron, Deta Gasser, Trond Slagstad and an anonymous reviewer are thanked for thorough and constructive reviews that improved the quality of the manuscript. This work was supported by the Research Council of Norway through its Centres of Excellence funding scheme, project number 223272 and funded by Grant 250327/F20 from the Research Council of Norway to the project "Hyperextension in magma-poor and magma-rich domains along the pre-Caledonian passive margin of Baltica". Sarek, Rohkunborri and Dividalen national parks are gratefully acknowledged for allowing helicopter transport and sampling within the parks' boundaries.

References

Abdelmalak, M.M., Andersen, T.B., Planke, S., Faleide, J.I., Corfu, F., Tegner, C., Shephard, G.E., Zastrozhnov, D. & Myklebust, R. 2015: The ocean-continent transition in the mid-Norwegian margin: Insight from seismic data and an onshore Caledonian field analogue. *Geology 43*, 1011–1014. https://doi.org/10.1130/G37086.1.

Åhäll, K.-I. & Connelly, J.N. 2008: Long-term convergence along SW Fennoscandia: 330 my of Proterozoic crustal growth. *Precambrian Research 161*, 452–474. https://doi.org/10.1016/j.precamres.2007.09.007.

Albrecht, L.G. 2000: *Early structural and metamorphic evolution of the Scandinavian Caledonides: a study of the eclogite-bearing Seve Nappe Complex at the Arctic Circle, Sweden*. PhD thesis, Lund University, Sweden, 132 pp.

Allen, P.A., Bowring, S., Leather, J., Brasier, M., Cozzi, A., Grotzinger, J.P., McCarron, G. & Amthor, J.E. 2002: Chronology of Neoproterozoic glaciations: new insights from Oman. *The 16th International Sedimenetological Congress, Abstract Volume, Johannesburg, South Africa*, p. 7–8.

Allen, P.A. & Etienne, J.L. 2008: Sedimentary challenge to Snowball Earth. *Nature Geoscience 1*, 817. https://doi.org/10.1038/ngeo355.

Andersen, T. 2005: Detrital zircons as tracers of sedimentary provenance: limiting conditions from statistics and numerical simulation. *Chemical Geology 216,* 249–270. https://doi.org/10.1016/j.chemgeo.2004.11.013.

Andersen, T.B., Corfu, F., Labrousse, L. & Osmundsen, P.-T. 2012: Evidence for hyper-extension along the pre-Caledonian margin of Baltica. *Journal of the Geological Society 169,* 601–612. https://doi.org/10.1144/0016-76492012-011.

Andersen, T., Kristoffersen, M. & Elburg, M.A. 2016: How far can we trust provenance and crustal evolution information from detrital zircons? A South African case study. *Gondwana Research 34*, 129–148. https://doi.org/10.1016/j.gr.2016.03.003.

Andersen, T., Kristoffersen, M. & Elburg, M.A. 2018: Visualizing, interpreting and comparing detrital zircon age and Hf isotope data in basin analysis – a graphical approach. *Basin Research 30*, 132–147. https://doi.org/10.1111/bre.12245.

Andréasson, P.-G. 1986: The Sarektjåkkå Nappe, Seve terranes of the northern Swedish Caledonides. *Geologiska Föreningen i Stockholm Förhandlingar 108,* 263–266. https://doi.org/10.1080/11035898609454697.

Andréasson, P. 1994: The Baltoscandian margin in Neoproterozoic-early Palaeozoic times. Some constraints on terrane derivation and accretion in the Arctic Scandinavian Caledonides. *Tectonophysics 231,* 1–32. https://doi.org/10.1016/0040-1951(94)90118-X.

Andréasson, P.-G., Svenningsen, O.M. & Albrecht, L. 1998: Dawn of Phanerozoic orogeny in the North Atlantic tract; evidence from the Seve-Kalak Superterrane, Scandinavian Caledonides. *Geologiska Föreningen i Stockholm Förhandlingar 120*, 159–172. https://doi.org/10.1080/11035899801202159.

Andréasson, P.-G., Allen, A., Aurell, O., Boman, D., Ekestubbe, J., Goerke, U., Lundgren, A., Nilsson, P. & Sandelin, S. 2018: Seve terranes of the Kebnekaise Mts., Swedish Caledonides, and their amalgamation, accretion and affinity. *Geologiska Föreningen i Stockholm Förhandlingar 140,* 264–291. https://doi.org/10.1080/11035897.2018.1470200.

Austrheim, H. & Corfu, F. 2009: Formation of planar deformation features (PDFs) in zircon during coseismic faulting and an evaluation of potential effects on U–Pb systematics. *Chemical Geology 261*, 25–31. https://doi.org/10.1016/j.chemgeo.2008.09.012.

Baird, G.B., Figg, S.A. & Chamberlain, K.R. 2014: Intrusive age and geochemistry of the Kebne Dyke Complex in the Seve Nappe Complex, Kebnekaise Massif, arctic Sweden Caledonides. *Geologiska Föreningen i Stockholm Förhandlingar 136*, 556–570. https://doi.org/10.1080/11035897.2014.924553.

Be'eri-Shlevin, Y., Gee, D., Claesson, S., Ladenberger, A., Majka, J., Kirkland, C., Robinson, P. & Frei, D. 2011: Provenance of Neoproterozoic sediments in the Särv nappes (Middle Allochthon) of the Scandinavian Caledonides: LA-ICP-MS and SIMS U–Pb dating of detrital zircons. *Precambrian Research 187,* 181–200. https://doi.org/10.1016/j.precamres.2011.03.007.

Beltrando, M., Manatschal, G., Mohn, G., Dal Piaz, G.V., Brovarone, A.V. & Masini, E. 2014: Recognizing remnants of magma-poor rifted margins in high-pressure orogenic belts: The Alpine case study. *Earth-Science Reviews 131*, 88–115.

Bertrand-sarfati, J. & Siedlecka, A. 1980: Columnar stromatolites of the terminal Precambrian Porsanger Dolomite and Grasdal Formation of Finnmark, north Norway. *Norsk Geologisk Tidsskrift 60*, 1–27.

Bingen, B. & Solli, A. 2009: Geochronology of magmatism in the Caledonian and Sveconorwegian belts of Baltica: synopsis for detrital zircon provenance studies. *Norwegian Journal of Geology 89*, 267–290.

Bingen, B., Demaiffe, D. & Breemen, O.V. 1998: The 616 Ma old Egersund basaltic dike swarm, SW Norway, and late Neoproterozoic opening of the Iapetus Ocean. *The Journal of Geology 106*, 565–574. https://doi.org/10.1086/516042.

Bingen, B., Griffin, W.L., Torsvik, T.H. & Saeed, A. 2005: Timing of Late Neoproterozoic glaciation on Baltica constrained by detrital zircon geochronology in the Hedmark Group, south-east Norway. T*erra Nova 17*, 250–258. https://doi.org/10.1111/j.1365-3121.2005.00609.x.

Bingen, B., Davis, W.J., Hamilton, M.A., Engvik, A.K., Stein, H.J., Skar, O. & Nordgulen, O. 2008: Geochronology of high-grade metamorphism in the Sveconorwegian belt, S. Norway: U-Pb, Th-Pb and Re-Os data. *Norwegian Journal of Geology 88,* 13–42.

Björklund, L. 1985: The Middle and Lower Allochthons in the Akkajaure-Tysfjord Area, northern Scandinavian Caledonides. *The Caledonide Orogen—Scandinavia and Related Areas*, 515–528.

Björklund, L. 1989: *Geology of the Akkajaure-Tysfjord-Lofoten Traverse, N. Scandinavian Caledonides.* PhD thesis, University of Technology and University of Göteborg, 214 pp.

Bowring, S., Myrow, P., Landing, E., Ramezani, J. & Grotzinger, J. 2003: Geochronological constraints on terminal Neoproterozoic events and the rise of Metazoan. *Abstract, EGS-AGU-EUG Joint Assembly,* 6–11 April, Nice, France.

Caby, R. & Bertrand-Sarfati, J. 1976: Carbonates et stromalolites du sommet du Groupe d'Eleonore Bay (Précambrien terminal) au Canning Land (Groenland oriental). *Grønlands geologiske undersøgelse Bulletin,* 1–51.

Corfu, F., Hanchar, J.M., Hoskin, P.W.O. & Kinny, P. 2003: Atlas of Zircon Textures. *Reviews in Mineralogy and Geochemistry 53*, 469–500. https://doi.org/10.2113/0530469.

Corfu, F., Roberts, R.J., Torsvik, T., Ashwal, L.D. & Ramsay, D.M. 2007: Peri-Gondwanan elements in the Caledonian nappes of Finnmark, Northern Norway: Implications for the Paleogeographic framework of the Scandinavian Caledonides. *American Journal of Science 307*, 434–458. https://doi.org/10.2475/02.2007.05.

Corfu, F., Andersen, T. & Gasser, D. 2014: The Scandinavian Caledonides: main features, conceptual advances and critical questions. *Geological Society, London, Special Publications 390*, 9–43. https://doi.org/10.1144/SP390.25.

Creveling, J.R., Bergmann, K.D. & Grotzinger, J.P. 2016: Cap carbonate platform facies model, Noonday Formation, SE California. *Geological Society of America Bulletin 128*, 1249–1269. https://doi.org/10.1130/B31442.1.

Dallmeyer, R., Andréasson, P. & Svenningsen, O. 1991: Initial tectonothermal evolution within the Scandinavian Caledonide accretionary prism: constraints from 40Ar/39Ar mineral ages within the Seve Nappe Complex, Sarek Mountains, Sweden. *Journal of Metamorphic Geology 9*, 203–218. https://doi.org/10.1111/j.1525-1314.1991.tb00515.x.

Dempster, T., Hay, D. & Bluck, B. 2004: Zircon growth in slate. *Geology 32*, 221–224. https://doi.org/10.1130/G20156.1.

Edwards, M. 1984: Sedimentology of the Upper Proterozoic glacial record, Vestertana Group, Finnmark, North Norway. *Norges geologiske undersøkelse Bulletin 394*, 1-76.

Edwards, M. 1986: Glacial environments. *Sedimentary environments and facies*, 445–470.

Epin, M.-E., Manatschal, G. & Amann, M. 2017: Defining diagnostic criteria to describe the role of rift inheritance in collisional orogens: the case of the Err-Platta nappes (Switzerland). *Swiss Journal of Geosciences 110*, 419–438. https://doi.org/10.1007/s00015-017-0271-6.

Eyles, N. & Januszczak, N. 2004: 'Zipper-rift': a tectonic model for Neoproterozoic glaciations during the breakup of Rodinia after 750 Ma. *Earth-Science Reviews 65,* 1–73. https://doi.org/10.1016/S0012-8252(03)00080-1.

Gasser, D., Jeřábek, P., Faber, C., Stünitz, H., Menegon, L., Corfu, F., Erambert, M. & Whitehouse, M. 2015: Behaviour of geochronometers and timing of metamorphic reactions during deformation at lower crustal conditions: phase equilibrium modelling and U–Pb dating of zircon, monazite, rutile and titanite from the Kalak Nappe Complex, northern Norway. *Journal of Metamorphic Geology 33*, 513–534. https://doi.org/10.1111/jmg.12131.

Gee, D.G., Ladenberger, A., Dahlqvist, P., Majka, J., Be'eri-Shlevin, Y., Frei, D. & Thomsen, T. 2014: The Baltoscandian margin detrital zircon signatures of the central Scandes. *Geological Society, London, Special Publications 390*, 131–155. https://doi.org/10.1144/SP390.20.

Gilotti, J.A. & Kumpulainen, R.A. 1986: Strain softening induced ductile flow in the Särv thrust sheet, Scandinavian Caledonides. *Journal of Structural Geology 8*, 441–455. https://doi.org/10.1016/0191-8141(86)90062-3.

Gorbatschev, R. 2004: The Transscandinavian Igneous Belt-introduction and background. *Special paper-Geological survey of Finland 37*, 1–9.

Halverson, G.P., Maloof, A.C. & Hoffman, P.F. 2004: The Marinoan glaciation (Neoproterozoic) in northeast Svalbard. *Basin Research 16*, 297–324. https://doi.org/10.1016/0191-8141(86)90062-3.

Halverson, G.P., Hoffman, P.F., Schrag, D.P., Maloof, A.C. & Rice, A.H.N. 2005: Toward a Neoproterozoic composite carbon-isotope record. *Geological Society of America Bulletin 117*, 1181–1207. https://doi.org/10.1130/B25630.1.

Hoffman, P.F. & Schrag, D.P. 2002: The snowball Earth hypothesis: testing the limits of global change. *Terra Nova 14*, 129–155. https://doi.org/10.1046/j.1365-3121.2002.00408.x.

Hoffman, P.F., Kaufman, A.J., Halverson, G.P. & Schrag, D.P. 1998: A Neoproterozoic snowball earth. *Science 281*, 1342–1346. https://doi.org/10.1126/science.281.5381.1342.

Hoffmann, K.-H., Condon, D., Bowring, S. & Crowley, J. 2004: U-Pb zircon date from the Neoproterozoic Ghaub Formation, Namibia: constraints on Marinoan glaciation. *Geology 3*2, 817–820. https://doi.org/10.1130/G20519.1.

Holtedahl, O. 1922: A tillite-like conglomerate in the Eocambrian Sparagmite of southern Norway. *American Journal of Science 4*, 165–173. https://doi.org/10.2475/ajs.s5-4.20.165.

Hyde, W.T., Crowley, T.J., Baum, S.K. & Peltier, W.R. 2000: Neoproterozoic 'snowball Earth' simulations with a coupled climate/ice-sheet model. *Nature 405*, 425–429. https://doi.org/10.1038/35013005.

Jakob, J., Alsaif, M., Corfu, F. & Andersen, T.B. 2017: Age and origin of thin discontinuous gneiss sheets in the distal domain of the magma-poor hyperextended pre-Caledonian margin of Baltica, southern Norway. *Journal of the Geological Society 174*, 557–571. https://doi.org/10.1144/jgs2016-049.

Jakob, J., Andersen, T.B. & Kjøll, H.J. 2019: A review and reinterpretation of the architecture of the South and South-Central Scandinavian Caledonides—A magma-poor to magma-rich transition and the significance of the reactivation of rift inherited structures. *Earth-Science Reviews 197*, 513–528. https://doi.org/10.1016/j.earscirev.2019.01.004.

Kathol, B. 1989: Evolution of the rifted and subducted late proterozoic to early Paleozoic Baltoscandian margin in the Torneträsk section, northern Swedish Caledonides. *Stockholm Contributions in Geology 42*, 1–83.

Kendall, B., Creaser, R.A. & Selby, D. 2006: Re-Os geochronology of postglacial black shales in Australia: Constraints on the timing of "Sturtian" glaciation. *Geology 34,* 729–732. https://doi.org/10.1130/G22775.1.

Kirkland, C.L., Daly, J.S. & Whitehouse, M.J. 2006: Granitic magmatism of Grenvillian and late Neoproterozoic age in Finnmark, Arctic Norway - Constraining pre-Scandian deformation in the Kalak Nappe Complex. *Precambrian Research 145*, 24–52. https://doi.org/10.1016/j.precamres.2005.11.012.

Kirkland, C.L., Bingen, B., Whitehouse, M., Beyer, E. & Griffin, W. 2011: Neoproterozoic palaeogeography in the North Atlantic Region: inferences from the Akkajaure and Seve Nappes of the Scandinavian Caledonides. *Precambrian Research 186*, 127–146. https://doi.org/10.1016/j.precamres.2011.01.010.

Kirschvink, J.L. 1992: Late Proterozoic low-latitude global glaciation: the snowball Earth. In Schopf, J.W. & Klein, C. (eds.): *The Proterozoic Biosphere*, Cambridge University Press, Cambridge, pp. 51–52.

Kjøll, H.J., Viola, G., Menegon, L. & Sørensen, B.E. 2015: Brittle–viscous deformation of vein quartz under fluid-rich low greenschist facies conditions. *Solid Earth Discussions 7*, 213–257. https://doi.org/10.5194/sed-7-213-2015.

Kjøll, H.J., Andersen, T.B., Corfu, F., Labrousse, L., Tegner, C., Abdelmalak, M.M. & Planke, S. 2019a: Timing of break-up and thermal evolution of a pre-Caledonian Neoproterozoic exhumed magma-rich rifted margin. *Tectonics 38.* https://doi.org/10.1029/2018TC005375.

Kjøll, H.J., Galland, O., Labrousse, L. & Andersen, T.B. 2019b: Emplacement mechanisms of a dyke swarm across the Brittle-Ductile transition and the geodynamic implications for magma-rich margins. E*arth and Planetary Science Letters 518*, 223–235. https://doi.org/10.5194/egusphere-egu2020-8215.

Kristoffersen, M., Andersen, T., Elburg, M.A. & Watkeys, M.K. 2016: Detrital zircon in a supercontinental setting: locally derived and far-transported components in the Ordovician Natal Group, South Africa. *Journal of the Geological Society 173,* 203–215. https://doi.org/10.1144/jgs2015-012.

Kumpulainen, R.A. 1980: Upper Proterozoic stratigraphy and depositional environments of the Tossåsfjället Group, Särv Nappe, southern Swedish Caledonides. *Geologiska Föreningen i Stockholm Förhandlingar 102*, 531–550. https://doi.org/10.1080/11035898009454506.

Kumpulainen, R.A. 2011: Chapter 61 The Neoproterozoic glaciogenic Lillfjället Formation, southern Swedish Caledonides. *Geological Society, London, Memoirs 36*, 1–629. https://doi.org/10.1144/M36.61.

Kumpulainen, R.A. & Nystuen, J.P. 1985: Late Proterozoic basin evolution and sedimentation in the westernmost part of Baltoscandia. *The Caledonide Orogen—Scandinavia and Related Areas 1*, 213–245.

Kumpulainen, R.A. & Greiling, R.O. 2011: Chapter 60 Evidence for late Neoproterozoic glaciation in the central Scandinavian Caledonides. *Geological Society, London, Memoirs 36*. https://doi.org/10.1144/M36.60.

Kumpulainen, R.A., Hamilton, M.A., Söderlund, U. & Nystuen, J.P. 2016: A new U-Pb baddeleyite age for the Ottfjället dolerite dyke swarm in the Scandinavian Caledonides - a minimum age for late Neoproterozoic glaciation in Baltica. *Abstracts of the 32nd Nordic Geologic Winter Meeting, 13–15 January, Helsinki, Finland.*

Ladenberger, A., Be, eri-Shlevin, Y., Claesson, S., Gee, D.G., Majka, J. & Romanova, I.V. 2014: Tectono-metamorphic evolution of the Åreskutan Nappe – Caledonian history revealed by SIMS U–Pb zircon geochronology. *Geological Society, London, Special Publications 390*, 337. https://doi.org/10.1144/SP390.10.

Larson, S.Å. & Berglund, J. 1992: A chronological subdivision of the Transscandinavian Igneous Belt—three magmatic episodes? *Geologiska Föreningen i Stockholm Förhandlingar 114*, 459–461. https://doi.org/10.1080/11035899209453912.

Le Heron, D.P. & Vandyk, T.M. 2019: A slippery slope for Cryogenian diamictites? T*he Depositional Record 5*, 306–321. https://doi.org/10.1002/dep2.67.

Le Heron, D.P., Hogan, K.A., Phillips, E.R., Huuse, M., Busfield, M.E. & Graham, A.G.C. 2019: An introduction to glaciated margins: the sedimentary and geophysical archive. *Geological Society, London, Special Publications 475,* 1–8. https://doi.org/10.1144/SP475.12.

Li, Z.X., Bogdanova, S.V., Collins, A.S., Davidson, A., De Waele, B., Ernst, R.E., Fitzsimons, I.C.W., Fuck, R.A., Gladkochub, D.P., Jacobs, J., Karlstrom, K.E., Lu, S., Natapov, L.M., Pease, V., Pisarevsky, S.A., Thrane, K. & Vernikovsky, V. 2008b: Assembly, configuration, and break-up history of Rodinia: A synthesis. *Precambrian Research 160*, 179–210. https://doi.org/10.1016/j.precamres.2007.04.021.

Lindahl, I., Stevens, B.P. & Zwaan, K.B. 2005: The geology of the Vaddas area, Troms: a key to our understanding of the Upper Allochthon in the Caledonides of northern Norway. *Norges geologiske undersøkelse 445*.

Melezhik, V., Ihlen, P., Kuznetsov, A., Gjelle, S., Solli, A., Gorokhov, I., Fallick, A., Sandstad, J. & Bjerkgård, T. 2015: Pre-Sturtian (800–730 Ma) depositional age of carbonates in sedimentary sequences hosting stratiform iron ores in the Uppermost Allochthon of the Norwegian Caledonides: A chemostratigraphic approach. *Precambrian Research 261*, 272–299. https://doi.org/10.1016/j.precamres.2015.02.015.

Merdith, A.S., Collins, A.S., Williams, S.E., Pisarevsky, S., Foden, J.D., Archibald, D.B., Blades, M.L., Alessio, B.L., Armistead, S., Plavsa, D., Clark, C. & Müller, R.D. 2017: A full-plate global reconstruction of the Neoproterozoic. *Gondwana Research 50*, 84–134. https://doi.org/10.1016/j.gr.2017.04.001.

Mohn, G., Manatschal, G., Masini, E. & Müntener, O. 2011: Rift-related inheritance in orogens: a case study from the Austroalpine nappes in Central Alps (SE-Switzerland and N-Italy). *International Journal of Earth Sciences 100,* 937–961. https://doi.org/10.1007/s00531-010-0630-2.

Nystuen, J.P. 1969: On the paragenesis of chert and carbonate minerals in chert-bearing magnesitic dolomite from the Kvitvola Nappe, southern Norway. *Norges geologiske undersøkelse 258*, 66–78.

Nystuen, J.P. 1976: Late Precambrian Moelv tillite deposited on a discontinuity surface associated with a fossil ice wedge, Rendalen, southern Norway. *Norsk Geologisk Tidsskrift 56*, 29–50.

Nystuen, J.P. 1980: Stratigraphy of the Upper Proterozoic Engerdalen Group, Kvitvola Nappe, south-eastern Scandinavian Caledonides. *Geologiska Föreningen i Stockholm Förhandlingar 102*, 551–560. https://doi.org/10.1080/11035898009454507.
Nystuen, J.P. 1983: Nappe and thrust structures in the Sparagmite Region, southern Norway. *Norges geologiske undersøkelse 380,* 67–83.

Nystuen, J.P. & Lamminen, J.T. 2011: Chapter 59 Neoproterozoic glaciation of South Norway: from continental interior to rift and pericratonic basins in western Baltica. *Geological Society, London, Memoirs 36*, 613. https://doi.org/10.1144/M36.59.

Nystuen, J.P., Andresen, A., Kumpulainen, R.A. & Siedlecka, A. 2008: Neoproterozoic basin evolution in Fennoscandia, East Greenland and Svalbard. *Episodes 31*, 35–43.
https://doi.org/10.18814/epiiugs/2008/v31i1/006-

Nystuen, J.P., Kumpulainen, R.A., Söderlund, U. & Hamilton, M.A. 2016: The Varangerian/Marinoan glaciation in Scandinavia - new age constraints. *Abstracts of the 32nd Nordic Geological Winter Meeting, 13-15 January, Helsinki, Finland.*

Paulsson, O. & Andreasson, P.-G. 2002: Attempted break-up of Rodinia at 850 Ma: geochronological evidence from the Seve–Kalak Superterrane, Scandinavian Caledonides. *Journal of the Geological Society 159,* 751–761. https://doi.org/10.1144/0016-764901-156.

Pease, V., Daly, J., Elming, S.-Å., Kumpulainen, R., Moczydlowska, M., Puchkov, V., Roberts, D., Saintot, A. & Stephenson, R. 2008: Baltica in the Cryogenian, 850–630 Ma. *Precambrian Research 160*, 46–65. https://doi.org/10.1016/j.precamres.2007.04.015.

Plink-Björklund, P., Björklund, L. & Loorents, K.-J. 2005: Sedimentary documentation of the break-up of Rodinia, Offerdal Nappe, Swedish Caledonides. *Precambrian Research 136,* 1–26.
https://doi.org/10.1016/j.precamres.2004.08.007.

Pu, J.P., Bowring, S.A., Ramezani, J., Myrow, P., Raub, T.D., Landing, E., Mills, A., Hodgin, E. & Macdonald, F.A. 2016: Dodging snowballs: Geochronology of the Gaskiers glaciation and the first appearance of the Ediacaran biota. *Geology 44,* 955–958. https://doi.org/10.1130/G38284.1.

Rasmussen, B. 2005: Zircon growth in very low grade metasedimentary rocks: evidence for zirconium mobility at~ 250 C. *Contributions to Mineralogy and Petrology 150*, 146–155.
https://doi.org/10.1007/s00410-005-0006-y.

Rehnström, E.F. & Corfu, F. 2004: Palaeoproterozoic U–Pb ages of autochthonous and allochthonous granites from the northern Swedish Caledonides—regional and palaeogeographic implications. *Precambrian Research 132*, 363–378. https://doi.org/10.1016/j.precamres.2004.03.005.

Rehnström, E.F., Corfu, F. & Torsvik, T.H. 2002: Evidence of a Late Precambrian (637 Ma) deformational event in the Caledonides of northern Sweden. *The Journal of Geology 110*, 591–601.
https://doi.org/10.1086/341594 .

Reusch, H. 1891: Det Nordlige Norges geologi. Med bidrag af Dahll T., Corneliussen OA, med profiler og Dahll's Geologisk Kart over det nordlige Norge'(1: 1,000,000). *Norges geologiske undersøkelse 3.*
Riding, R. 2011: Microbialites, stromatolites, and thrombolites. *Encyclopedia of geobiology 635–654*. https://doi.org/10.1007/978-1-4020-9212-1_196.

Rimsa, A., Whitehouse, M., Johansson, L. & Piazolo, S. 2007: Brittle fracturing and fracture healing of zircon: An integrated cathodoluminescence, EBSD, U-Th-Pb, and REE study. *American Mineralogist 92*, 1213–1224. https://doi.org/10.2138/am.2007.2458.

Roberts, D. & Gee, D.G. 1985: An introduction to the structure of the Scandinavian Caledonides. *The Caledonide orogen–Scandinavia and related areas 1,* 55–68.

Root, D. & Corfu, F. 2012: U–Pb geochronology of two discrete Ordovician high-pressure metamorphic events in the Seve Nappe Complex, Scandinavian Caledonides. *Contributions to Mineralogy and Petrology 163,* 769–788. https://doi.org/10.1007/s00410-011-0698-0

Satkoski, A.M., Hietpas, J., Samson, S.D. & Wilkinson, B.H. 2013: Likeness among detrital zircon populations—An approach to the comparison of age frequency data in time and space. *Geological Society of America Bulletin 125*, 1783–1799. https://doi.org/10.1130/B30888.1.

Siedlecka, A., Roberts, D., Nystuen, J. & Olovyanishnikov, V. 2004: Northeastern and northwestern margins of Baltica in Neoproterozoic time: evidence from the Timanian and Caledonian Orogens. *Geological Society, London, Memoirs 30,* 169–190. https://doi.org/10.1144/GSL.MEM.2004.030.01.15.

Slagstad, T. & Kirkland, C.L. 2017: The use of detrital zircon data in terrane analysis: A nonunique answer to provenance and tectonostratigraphic position in the Scandinavian Caledonides. *Lithosphere 9*, 1002–1011. https://doi.org/10.1144/GSL.MEM.2004.030.01.15.

Slagstad, T., Kulakov, E., Kirkland, C.L., Roberts, N.M. & Ganerød, M. 2019: Breaking the Grenville–Sveconorwegian link in Rodinia reconstructions. *Terra Nova 31*, 430–437. https://doi.org/10.1111/ter.12406.

Sønderholm, M., Frederiksen, K.S., Smith, M.P. & Tirsgaard, H. 2008: Neoproterozoic sedimentary basins with glacigenic deposits of the East Greenland Caledonides. In Higgins, A.K., Gilotti, J.A. & Smith, M.P. (eds.): *The Greenland Caledonides: Evolution of the Northeast Margin of Laurentia,* Geological Society of America Memoirs 202, pp. 99–136. https://doi.org/10.1130/2008.1202(05).

Stølen, L.K. 1994: The rift-related mafic dyke complex of the Rohkunborri Nappe, Indre Troms, northern Norwegian Caledonides. *Norsk Geologisk Tidsskrift 74*, 35–47.

Svenningsen, O.M. 1994a: Tectonic significance of the meta-evaporitic magnesite and scapolite deposits in the Seve Nappes, Sarek Mts., Swedish Caledonides. *Tectonophysics 231,* 33–44. https://doi.org/10.1016/0040-1951(94)90119-8.

Svenningsen, O.M. 1994b: The Baltica–Iapetus passive margin dyke complex in the Sarektjåkkå Nappe, northern Swedish Caledonides. *Geological Journal 29*, 323–354. https://doi.org/10.1002/gj.3350290403.

Svenningsen, O.M. 1995: Extensional deformation along the Late Precambrian-Cambrian Baltoscandian passive margin: the Sarektjåkkå Nappe, Swedish Caledonides. *Geologische Rundschau 84,* 649–664. https://doi.org/10.1007/s005310050031.

Svenningsen, O.M. 2000: Thermal history of thrust sheets in an orogenic wedge: 40Ar/39Ar data from the polymetamorphic Seve Nappe Complex, northern Swedish Caledonides. *Geological Magazine 137,* 437–446. https://doi.org/10.1017/S0016756800004210.

Svenningsen, O.M. 2001: Onset of seafloor spreading in the Iapetus Ocean at 608 Ma: precise age of the Sarek Dyke Swarm, northern Swedish Caledonides. *Precambrian Research 110*, 241–254. https://doi.org/10.1016/S0301-9268(01)00189-9.

Tegner, C., Andersen, T.B., Kjøll, H.J., Brown, E.L., Hagen-Peter, G., Corfu, F., Planke, S. & Torsvik, T. 2019: A mantle Plume origin for the Scandinavian Dyke Complex: a "piercing point" for the 615 Ma plate reconstruction of Baltica? *Geochemistry, Geophysics, Geosystems 20*, 1075–1094. https://doi.org/10.1029/2018GC007941.

Vermeesch, P. 2018: IsoplotR: A free and open toolbox for geochronology. *Geoscience Frontiers 9*, 1479–1493. https://doi.org/10.1016/j.gsf.2018.04.001.

Vidal, G. 1976: *Late Precambrian microfossils from the Visingso Beds in southern Sweden.* Universitetsforlaget, 8200094189.

Walderhaug, H.J., Torsvik, T.H., Eide, E.A., Sundvoll, B. & Bingen, B. 1999: Geochronology and palaeomagnetism of the Hunnedalen dykes, SW Norway: implications for the Sveconorwegian apparent polar wander loop. *Earth and Planetary Science Letters 169*, 71–83. https://doi.org/10.1016/S0012-821X(99)00066-7

Zhang, W., Roberts, D. & Pease, V. 2016: Provenance of sandstones from Caledonian nappes in Finnmark, Norway: implications for Neoproterozoic and Cambrian palaeogeography. *Tectonophysics 691*, 198-205.

Zwaan, B.K. & van Roermund, H.L. 1990: A rift-related mafic dyke swarm in the Corrovarre Nappe of the Caledonian Middle Allochthon, Troms, North Norway, and its tectonometamorphic evolution. *Norges Geologiske Undersøkelse Bulletin 419*, 25–44.

Zwaan, K., Cramer, J. & Ryghaug, P. 1975: Prospekteringskartlegging i Kvænangen, Troms fylke. *Unpublished NGU-rapport 76*.